



Polarized gamma-gamma collisions in the ReneSANCe event generator

Renat Sadykov, Vitaly Yermolchyk
(DLNP JINR)

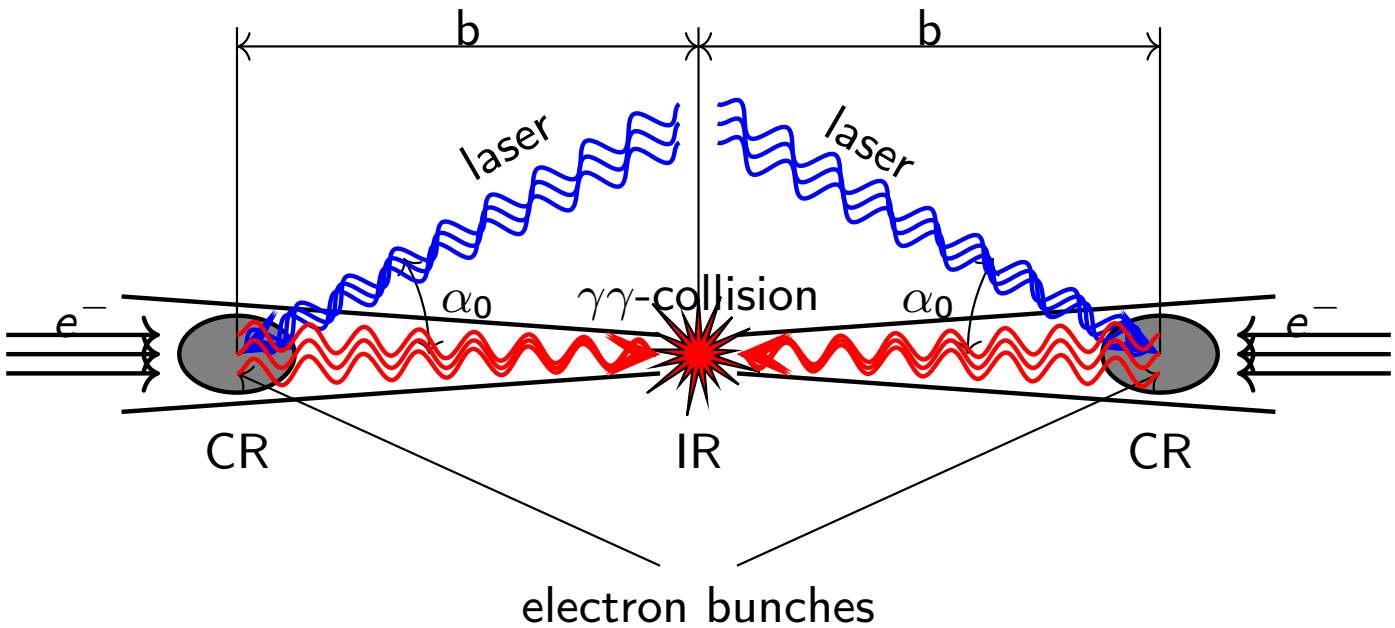
CEPC International Workshop
Shanghai, October 26th, 2026

Motivation

- New opportunities for physics of photon-photon collisions are associated with the future high-energy e^+e^- collider operated in $\gamma\gamma$-mode, e.g., through inverse Compton backscattering (ICS) of laser photons
- Photon colliders have high potential in:
  - Higgs physics
  - Gauge boson physics
  - Hadron physics and QCD
  - New physics beyond SM
- The direct observation of collisions of real photons is expected at photon collider with collision energy ~ 1 MeV
  (`Genie` collider in Shenzhen, China)
- Polarization effects can be studied by varying polarization states of initial electron and laser photon beams

Photon collider based on ee collider

$e \to \gamma$ conversion through the ICS of laser light on high-energy electrons (I.F. Ginzburg, G.L. Kotkin, V.G. Serbo and V.I. Telnov. ZhETF Pis'ma. 34 (1981) 514):



Basic parameters:

- $x_0 = \frac{4E\omega_0}{m_e^2}$, where E – electron energy, ω_0 – the laser photon energy
- P_e – electron beam long. polarization, P_γ – laser beam circ. polarization, P_t – laser beam linear polarization, Φ – azimuthal angle of lazer photon linear polarization
- $x = \frac{\omega}{E} \leqslant \frac{x_0}{1+x_0}$, where ω – energy of the back-scattered photon

Helicity density matrix for photons

- Circular polarization

$$\rho_\gamma^{circ} = 1/2 \begin{pmatrix} 1+\xi_2 & 0 \\ 0 & 1-\xi_2 \end{pmatrix} = 1/2 \begin{pmatrix} 1+\mathcal{P}^{circ} & 0 \\ 0 & 1-\mathcal{P}^{circ} \end{pmatrix}$$

  $\mathcal{P}^{circ} = \xi_2 \in [-1;1]$ is the *circular polarization degree* ($\mathcal{P}^{circ} = +1$ corresponds to photon with positive helicity $\lambda = +1$)

- Linear polarization

$$\rho_\gamma^{lin} = 1/2 \begin{pmatrix} 1 & -\xi_3 + i\xi_1 \\ -\xi_3 - i\xi_1 & 1 \end{pmatrix} = 1/2 \begin{pmatrix} 1 & -\mathcal{P}^{lin} e^{-2i\phi} \\ -\mathcal{P}^{lin} e^{2i\phi} & 1 \end{pmatrix}$$

  $\xi_1, \xi_3 \in [0;1]$, $\mathcal{P}^{lin} = \xi_{13} = \sqrt{\xi_1^2 + \xi_3^2} \in [0;1]$ is the *linear polarization degree*, $\phi = \frac{1}{2} Arg(\xi_1 - i\xi_3) \in [0;\pi]$ is the *linear polarization angle*.

Helicity density matrix for photons

- Mixed polarization

$$\rho^{\gamma} = 1/2 \begin{pmatrix} 1+\xi_2 & -\xi_3 + i\xi_1 \\ -\xi_3 - i\xi_1 & 1-\xi_2 \end{pmatrix} = 1/2 \begin{pmatrix} 1+\mathcal{P}^{circ} & -\mathcal{P}^{lin} e^{-2i\phi} \\ -\mathcal{P}^{lin} e^{2i\phi} & 1-\mathcal{P}^{circ} \end{pmatrix}$$

$\xi_1^2 + \xi_2^2 + \xi_3^2 = (\mathcal{P}^{circ})^2 + (\mathcal{P}^{lin})^2 \leqslant 1$, $\mathcal{P}^{lin} \geqslant 0$.

- The cross section for the process $\gamma\gamma \to X$ with polarized initial photons can be written as

$$d\sigma = \sum_{\lambda_1 \lambda_2 \lambda_1' \lambda_2'} \rho^{\gamma_1}_{\lambda_1 \lambda_1'} \rho^{\gamma_2}_{\lambda_2 \lambda_2'} \mathcal{H}^{\gamma\gamma \to X}_{\lambda_1 \lambda_2} \left(\mathcal{H}^{\gamma\gamma \to X}_{\lambda_1' \lambda_2'} \right)^{\dagger} d\Phi,$$

where $\mathcal{H}_{\lambda_1 \lambda_2}$ – helicity amplitudes for generic process $\gamma\gamma \to X$ summed over the helicities of the final particles:

$$\mathcal{H}^{\gamma\gamma \to X}_{\lambda_1 \lambda_2} \left(\mathcal{H}^{\gamma\gamma \to X}_{\lambda_1' \lambda_2'} \right)^{\dagger} = \sum_{\lambda_i} \mathcal{H}^{\gamma\gamma \to X}_{\lambda_1 \lambda_2 \ldots \lambda_i \ldots} \left(\mathcal{H}^{\gamma\gamma \to X}_{\lambda_1' \lambda_2' \ldots \lambda_i \ldots} \right)^{\dagger}$$

Density matrices for backscattered photons

$$\rho^{\gamma_1} = 1/2 \begin{pmatrix} 1+\xi_2^1(x_1) & -\xi_{13}^1(x_1)e^{-2i(\Phi_1-\phi)} \\ -\xi_{13}^1(x_1)e^{2i(\Phi_1-\phi)} & 1-\xi_2^1(x_1) \end{pmatrix},$$

$$\rho^{\gamma_2} = 1/2 \begin{pmatrix} 1+\xi_2^2(x_2) & -\xi_{13}^2(x_2)e^{2i(\Phi_2-\phi)} \\ -\xi_{13}^2(x_2)e^{-2i(\Phi_2-\phi)} & 1-\xi_2^2(x_2) \end{pmatrix}.$$

$$\xi_2^i(x_i) = \frac{P_e^i f_2(x_i) + P_\gamma^i f_3(x_i)}{C^i(x_i)}, \quad \xi_{13}(x_i) = \frac{2r^2(x_i)P_t^i}{C^i(x_i)}, \quad C^i(x_i) = f_0(x_i) + P_e^i P_\gamma^i f_1(x_i),$$

$$f_0(x_i) = \frac{1}{1+x_i} + 1 - x_i - 4r(x_i)(1-r(x_i)),$$

$$f_1(x_i) = \frac{x_i}{1-x_i}(1-2r(x_i))(2-x_i),$$

$$f_2(x_i) = x_0 r(x_i)\left[1+(1-x_i)(1-2r(x_i))^2\right],$$

$$f_3(x_i) = (1-2r(x_i))\left(\frac{1}{1-x_i}+1-x_i\right),$$

$$r(x_i) = \frac{x_i}{x_0(1-x_i)}.$$

Cross sections for $2 \to 2$ process

$$\frac{d\sigma_{\gamma\gamma\to X}}{dx_1\,dx_2\,d\cos\theta^*\,d\phi} = \frac{d\mathcal{L}_{\gamma\gamma}}{dx_1\,dx_2}\,\frac{d\hat{\sigma}_{\gamma\gamma\to X}}{d\cos\theta^*\,d\phi},$$

$$\frac{d\hat{\sigma}_{\gamma\gamma\to X}}{d\cos\theta^*\,d\phi} = \frac{N_{\gamma\gamma\to X}}{64\pi\hat{s}} \sum_{\lambda_1\lambda_2\lambda_1'\lambda_2'} \rho^{\gamma_1}_{\lambda_1\lambda_1'}\rho^{\gamma_2}_{\lambda_2\lambda_2'}\mathcal{H}^{\gamma\gamma\to X}_{\lambda_1\lambda_2}\left(\mathcal{H}^{\gamma\gamma\to X}_{\lambda_1'\lambda_2'}\right)^{\dagger},$$

$$N_{\gamma\gamma\to\gamma\gamma} = \frac{1}{2},$$

$$N_{\gamma\gamma\to Z\gamma} = 1 - \frac{M_Z^2}{\hat{s}},$$

$$N_{\gamma\gamma\to ZZ} = \frac{1}{2}\sqrt{1 - \frac{4M_Z^2}{\hat{s}}},$$

$$N_{\gamma\gamma\to e^-e^+} = \frac{1}{2}\sqrt{1 - \frac{4m_e^2}{\hat{s}}}.$$

Luminosity of backscattered photons

Luminosity distribution of colliding photons $\frac{d\mathcal{L}_{\gamma\gamma}}{dx_1\,dx_2}$ depends on the reduced distance ρ between conversion and collision points and aspect ratio A of horizontal σ_{ye} and vertical σ_{xe} sizes of electron beams (Ginzburg I. F., Kotkin G. L. Phys. J. C. 2000. V. 13. P. 295):

$$\rho^2 = \left(\frac{b}{(E/m_e)\sigma_{xe}}\right)^2 + \left(\frac{b}{(E/m_e)\sigma_{ye}}\right)^2, \quad A = \frac{\sigma_{xe}}{\sigma_{ye}}$$

$$\frac{d\mathcal{L}_{\gamma\gamma}}{dx_1\,dx_2} = \frac{1}{(2\pi)^2}\int d\phi_1 d\phi_2 f^1(x_0,x_1) f^2(x_0,x_2) \exp\left[-\frac{\rho^2\Psi}{4(1+A^2)}\right],$$

$$\Psi = A^2\left(g(x_0,x_1)\cos\phi_1 + g(x_0,x_2)\cos\phi_2\right)^2 + \left(g(x_0,x_1)\sin\phi_1 + g(x_0,x_2)\sin\phi_2\right)^2,$$

$$g(x_0,x_i) = \sqrt{\frac{x_0}{x_i} - x_0 - 1},$$

$$f^i(x_0,x_i) = N^i(x_0)\left[f_0(x_i) + P_e^i P_\gamma^i f_1(x_i)\right].$$

Cross sections for $\gamma\gamma \to \gamma\gamma, \gamma Z, ZZ, e^- e^+$ in SANC

The $\gamma\gamma \to \gamma\gamma, \gamma Z, ZZ$ SM processes through fermion and boson loops were calculated within the SANC framework:

- $\gamma\gamma \to \gamma\gamma$: D. Bardin, L. Kalinovskaya and E. Uglov. Physics of Atomic Nuclei, 2010, Vol. 73, No. 11, pp. 1878–1888
- $\gamma\gamma \to \gamma Z$: D. Bardin, L. Kalinovskaya and E. Uglov. Physics of Atomic Nuclei, 2013, Vol. 76, No. 11, pp. 1339–1344
- $\gamma\gamma \to ZZ$: D. Bardin et al. Physics of Particles and Nuclei Letters, 2017, Vol. 14, No. 6, pp. 811–816

The $\gamma\gamma \to e^- e^+(\gamma)$ process at 1-loop EW

Numerical results: input parameters

We performed numerical calculations in the $\alpha(0)$-scheme at $\sqrt{s} = 500$ GeV.
The results for $\rho = 0$ were cross-checked with SANCphot program.
Input parameters:

$$x_0 = 4.83,$$
$$\alpha = 1/137.035990996,$$

$M_Z = 91.1867$ GeV,	$M_W = 80.45149$ GeV,	$M_H = 125$ GeV,
$m_e = 0.51099907$ MeV,	$m_\mu = 0.105658389$ GeV,	$m_\tau = 1.77705$ GeV,
$m_d = 0.083$ GeV,	$m_s = 0.215$ GeV,	$m_b = 4.7$ GeV,
$m_u = 0.062$ GeV,	$m_c = 1.5$ GeV,	$m_t = 173.8$ GeV.

Polarization configurations:

- Set 1: $P_e^1 = P_e^2 = 0.8, P_\gamma^1 = P_\gamma^2 = -1, P_t^1 = P_t^2 = 0$
- Set 2: $P_e^1 = P_e^2 = 0, P_\gamma^1 = P_\gamma^2 = 0, P_t^1 = P_t^2 = 1, \Phi^1 = \Phi^2$
- Set 3: $P_e^1 = 0.8, P_e^2 = 0, P_\gamma^1 = -1, P_\gamma^2 = 0, P_t^1 = 0, P_t^2 = 1$

Cuts: $30^\circ < \theta < 150^\circ, M_{\gamma\gamma} > 20$ GeV, $M_{\gamma Z} > 100$ GeV, $M_{ZZ} > 200$ GeV.

Cross sections for $\gamma\gamma \to \gamma\gamma, \gamma Z, ZZ$ at $\sqrt{s} = 500$ GeV

$\gamma\gamma \to \gamma\gamma$

ρ	0	1	5
σ, fb [Set 1]	9.4420(1)	1.9820(1)	0.2232(1)
σ, fb [Set 2]	8.0452(2)	1.5473(1)	0.1448(1)
σ, fb [Set 3]	8.0134(2)	1.6429(1)	0.1647(1)

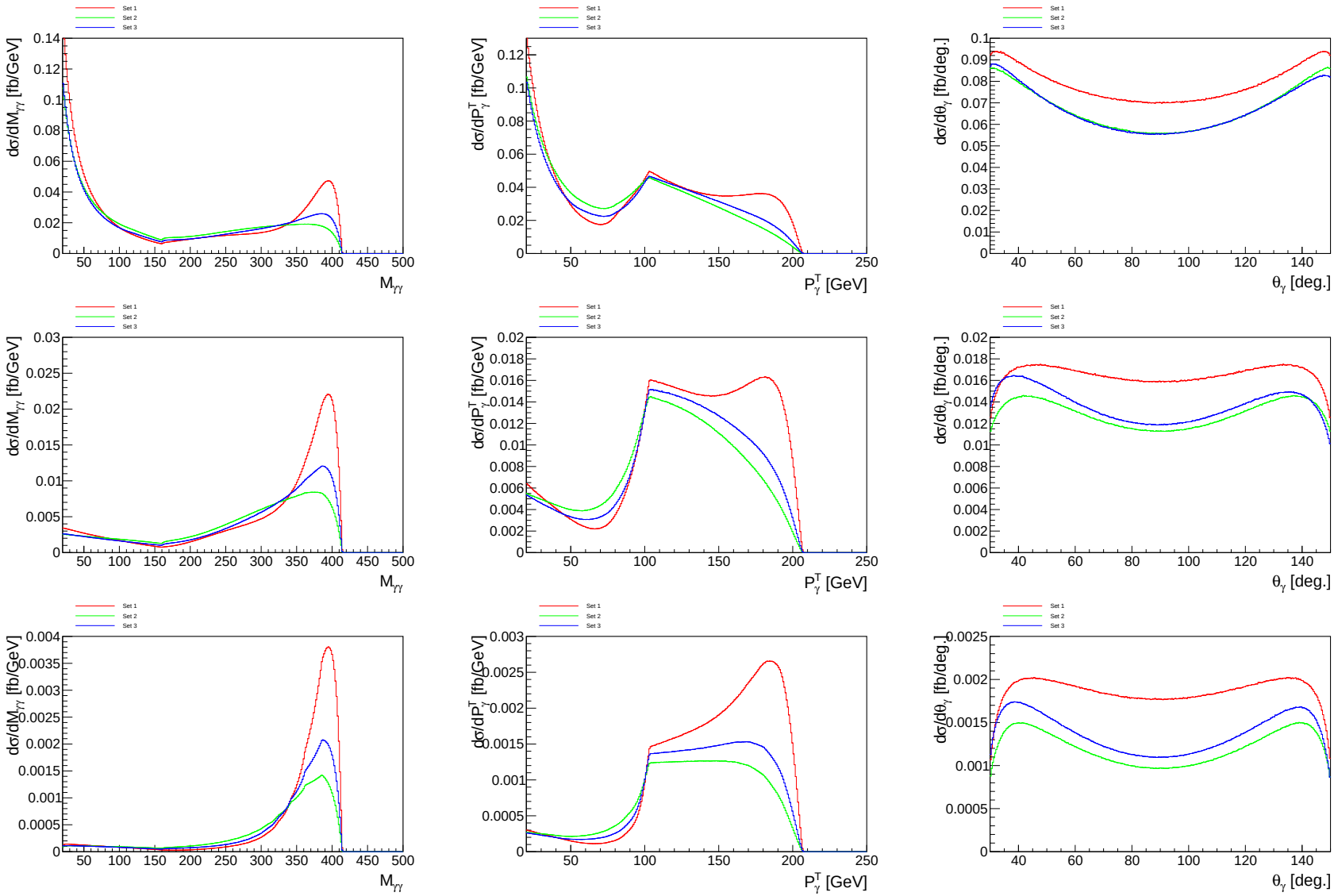
$\gamma\gamma \to \gamma Z$

ρ	0	1	5
σ, fb [Set 1]	21.528(1)	8.884(1)	1.247(1)
σ, fb [Set 2]	19.373(1)	7.196(1)	0.818(1)
σ, fb [Set 3]	17.015(1)	6.426(1)	0.750(1)

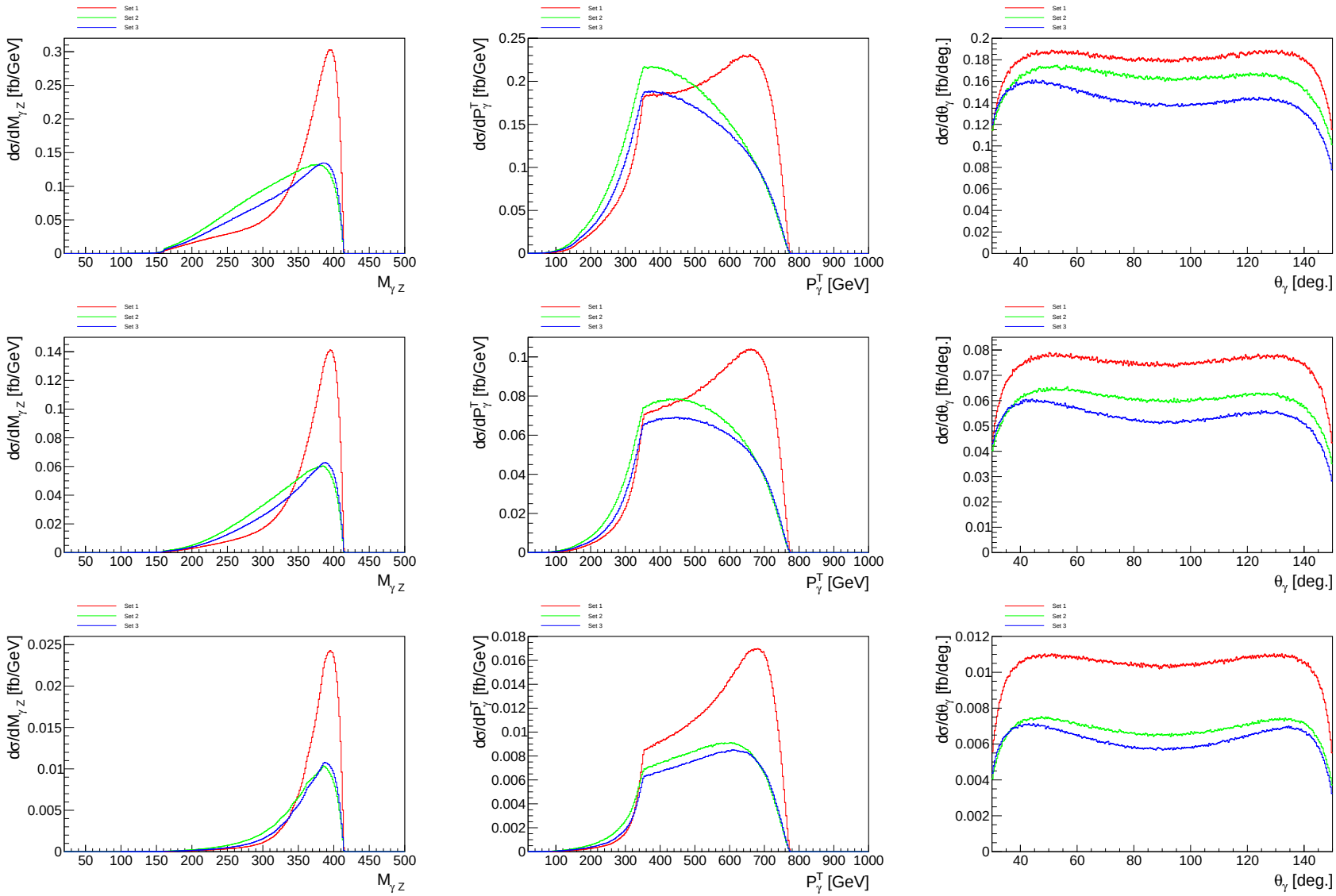
$\gamma\gamma \to ZZ$

ρ	0	1	5
σ, fb [Set 1]	32.326(1)	13.520(1)	1.898(1)
σ, fb [Set 2]	21.802(1)	8.361(1)	0.975(1)
σ, fb [Set 3]	24.312(1)	9.599(1)	1.176(1)

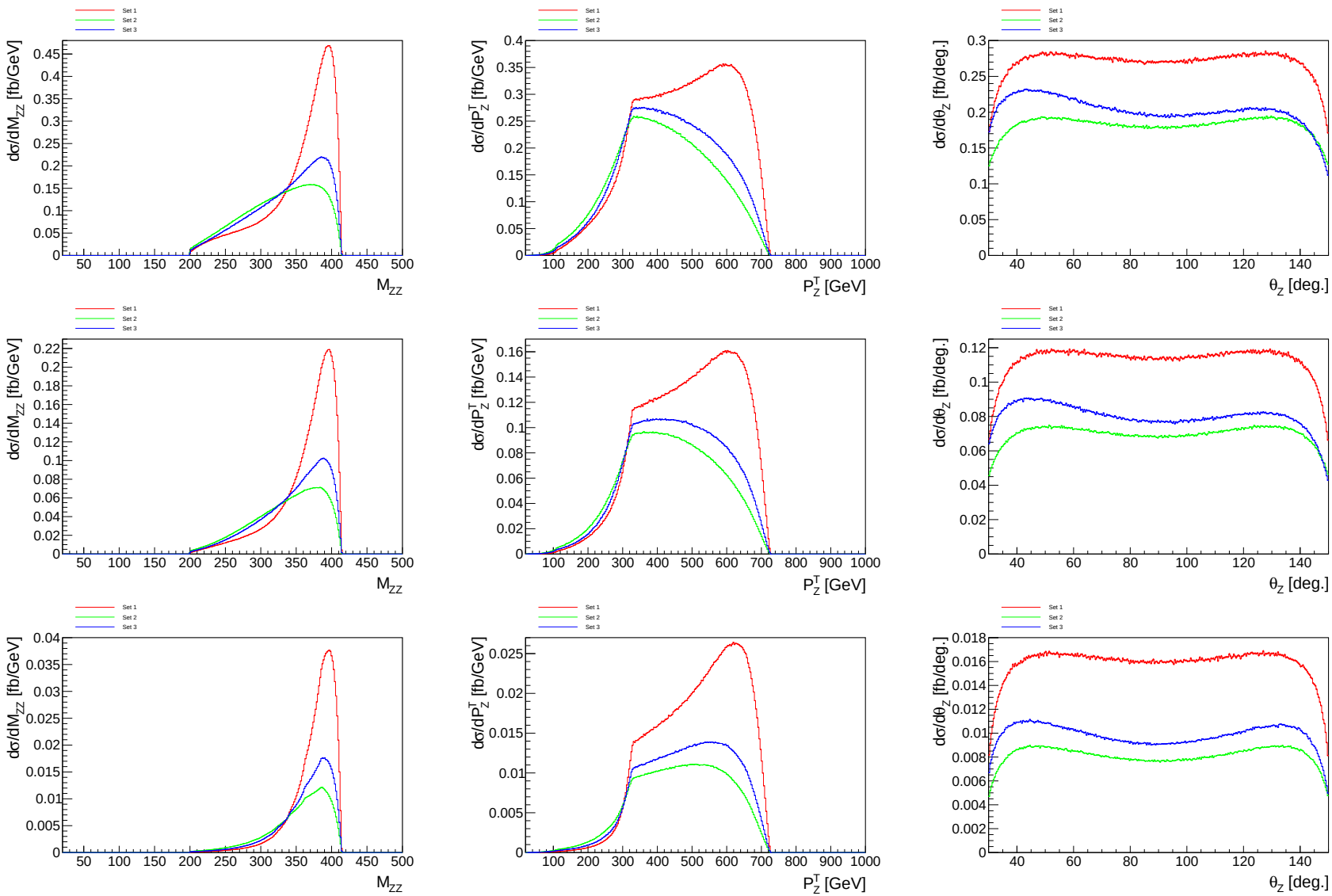
Distributions for $\gamma\gamma \to \gamma\gamma$ $(\rho = 0, 1, 5)$



Distributions for $\gamma\gamma \to \gamma Z$ $(\rho = 0, 1, 5)$

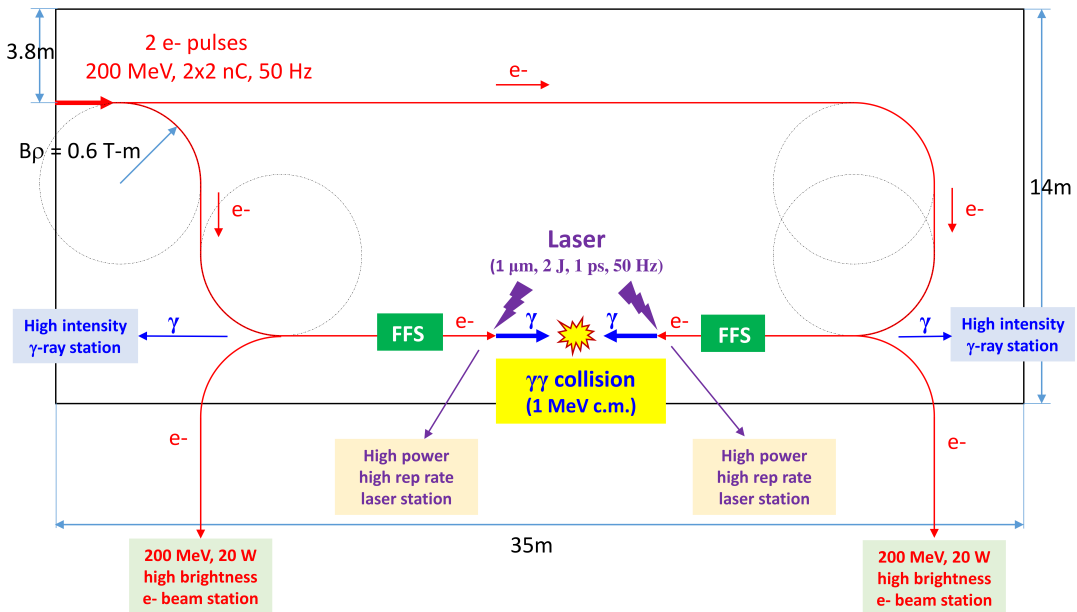


Distributions for $\gamma\gamma \to ZZ$ $(\rho = 0, 1, 5)$



Application for photon collider at $\sqrt{S_{\gamma\gamma}} \sim 1$ MeV

The photon collider Genie is proposed with $\sqrt{S_{\gamma\gamma}} \sim 1$ MeV
T. Takahashi et.al. Eur. Phys. J. C (2018) 78:893



Picture from Huang Yongshen presentation DOI:10.13140/RG.2.2.11301.88806

Application for photon collider at $\sqrt{S_{\gamma\gamma}} \sim 1$ MeV

Comparison of ReneSANCe and WHIZARD

- Set 1: unpolarized;
- Set 2: $(\pm, \pm)$;
- Set 3: $(\pm, \mp)$;
- Set 4: $(\phi_1 = 0, \phi_2 = 0)$;
- Set 5: $(\phi_1 = 0, \phi_2 = \pi/2)$ for $\gamma\gamma$ or $e^-\gamma$ in initial state, $(\phi_1 = 0, \phi_2 = \pi)$ for e^-e^- in initial state.

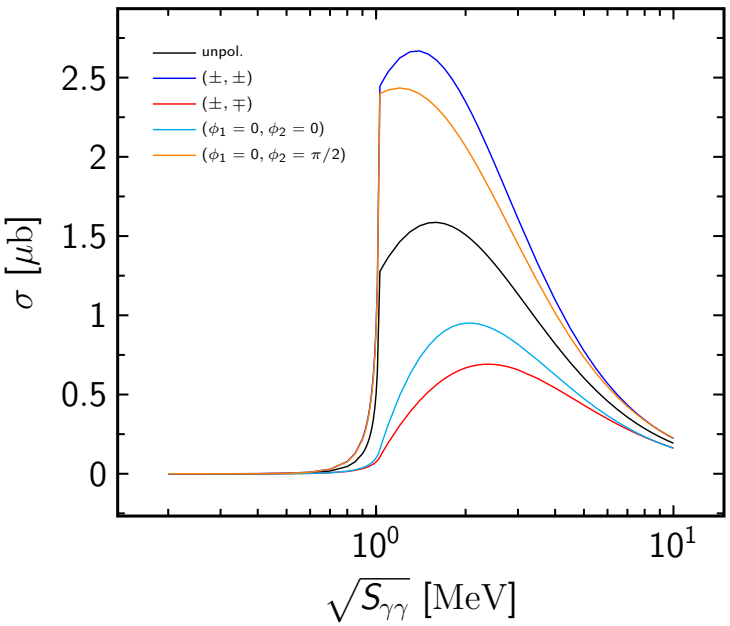
Process	σ [μb] Set 1	σ [μb] Set 2	σ [μb] Set 3	σ [μb] Set 4	σ [μb] Set 5
$\gamma\gamma \to \gamma\gamma$ (one-loop)	1.583(1)	2.648(1)	0.518(1)	0.807(1)	2.359(1)
$\gamma\gamma \to e^+e^-$	$1.636(1) \times 10^5$ $1.637(1) \times 10^5$	$1.968(1) \times 10^5$ $1.969(1) \times 10^5$	$1.305(1) \times 10^5$ $1.306(1) \times 10^5$	$1.339(1) \times 10^5$ $1.400(1) \times 10^5$	$1.934(1) \times 10^5$ $1.935(1) \times 10^5$
$\gamma\gamma \to e^+e^-$ (one-loop)	$1.620(1) \times 10^5$	$1.946(1) \times 10^5$	$1.294(1) \times 10^5$	$1.328(1) \times 10^5$	$1.912(1) \times 10^5$
$\gamma\gamma \to e^+e^-\gamma$	$3.759(1) \times 10^3$ $3.761(1) \times 10^3$	$4.614(1) \times 10^3$ $4.616(1) \times 10^3$	$2.904(1) \times 10^3$ $2.906(1) \times 10^3$	$3.103(1) \times 10^3$ $3.104(1) \times 10^3$	$4.415(1) \times 10^3$ $4.418(1) \times 10^3$
$e^-\gamma \to e^-\gamma$	$1.429(1) \times 10^5$ $1.430(1) \times 10^5$	$1.686(1) \times 10^5$ $1.687(1) \times 10^5$	$1.171(1) \times 10^5$ $1.172(1) \times 10^5$	$1.429(1) \times 10^5$ $1.429(1) \times 10^5$	$1.429(1) \times 10^5$ $1.429(1) \times 10^5$
$e^-\gamma \to e^-e^+e^-$	$1.147(1) \times 10^2$ $1.147(1) \times 10^2$	$1.517(1) \times 10^2$ $1.516(1) \times 10^2$	$0.777(1) \times 10^2$ $0.778(1) \times 10^2$	$1.147(1) \times 10^2$ $1.147(1) \times 10^2$	$1.147(1) \times 10^2$ $1.147(1) \times 10^2$
$e^-e^- \to e^-e^-$	$2.377(1) \times 10^7$ $2.379(1) \times 10^7$	$2.549(1) \times 10^7$ $2.550(1) \times 10^7$	$2.206(1) \times 10^7$ $2.207(1) \times 10^7$	$2.427(1) \times 10^7$ $2.428(1) \times 10^7$	$2.328(1) \times 10^7$ $2.329(1) \times 10^7$

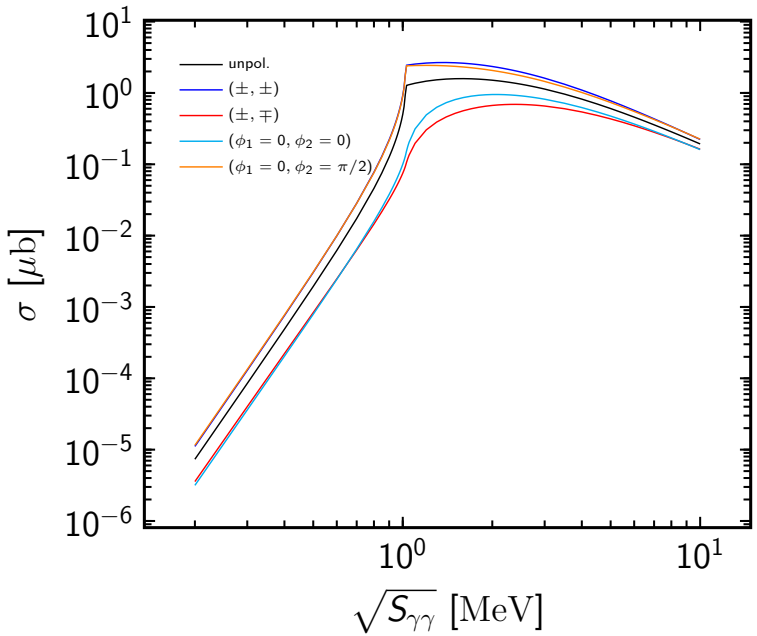
For these processes we applied the cut $|\cos\theta| < 0.9806$ for at least one of the final particles.

$e^-\gamma \to e^-e^+e^-$ process is calculated at $\sqrt{S} = 2$ MeV, other processes are evaluated at $\sqrt{S} = 1.5$ MeV.

Application for a photon collider at $\sqrt{S_{\gamma\gamma}} \sim 1$ MeV

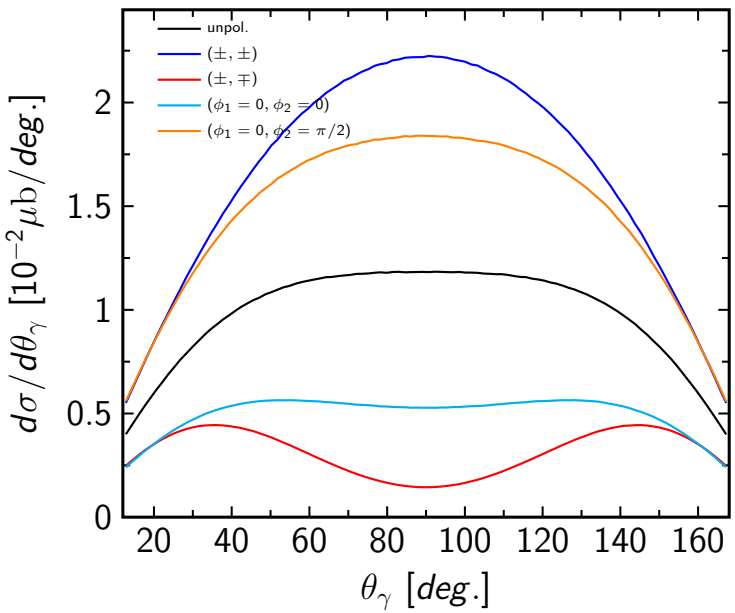
$\gamma\gamma \to \gamma\gamma$ cross sections for different polarization

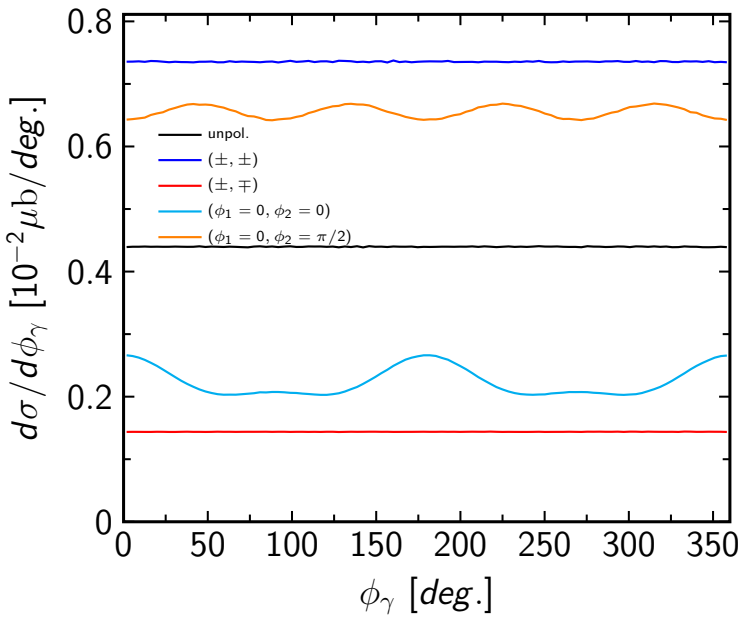




Application for a photon collider at $\sqrt{S_{\gamma\gamma}} \sim 1$ MeV

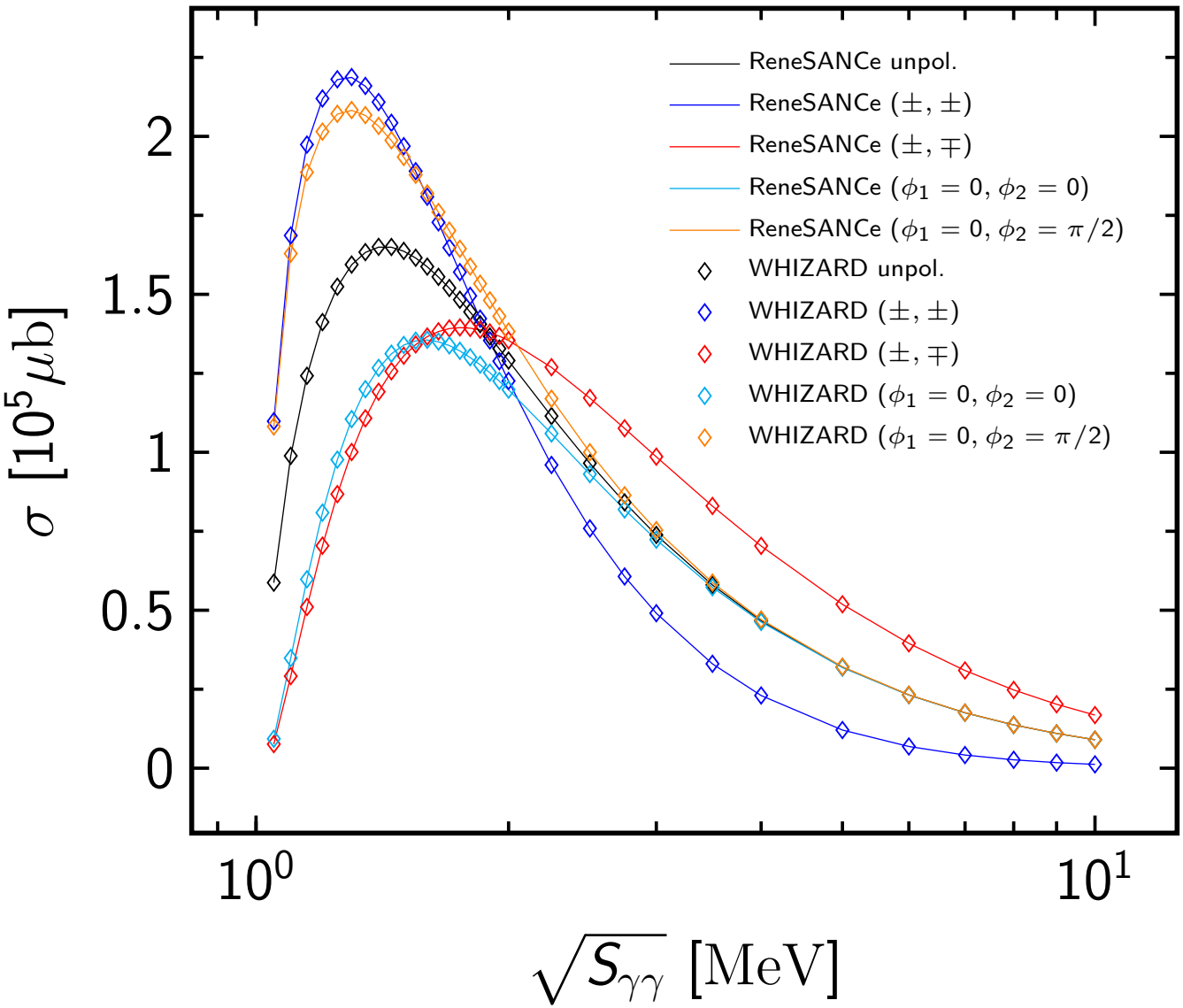
$\gamma\gamma \to \gamma\gamma$ cross sections for different polarization at $\sqrt{S_{\gamma\gamma}} = 1.5$ MeV





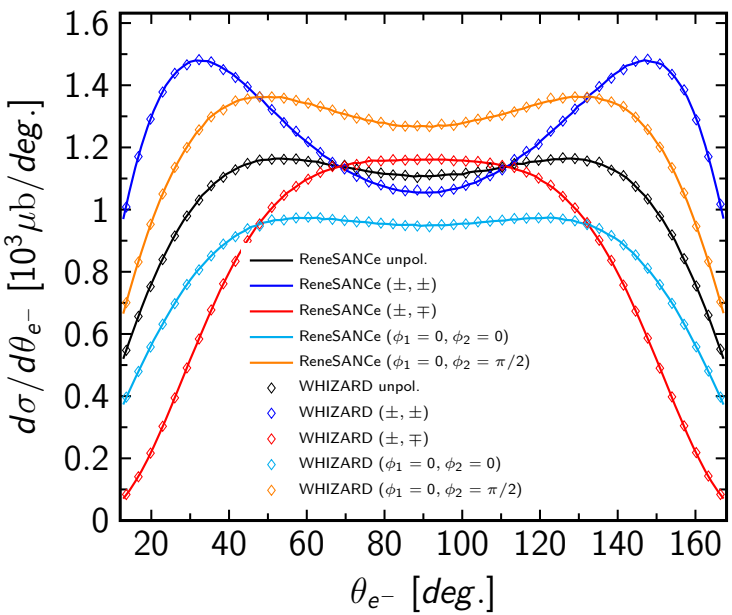
Application for a photon collider at $\sqrt{S_{\gamma\gamma}} \sim 1$ MeV

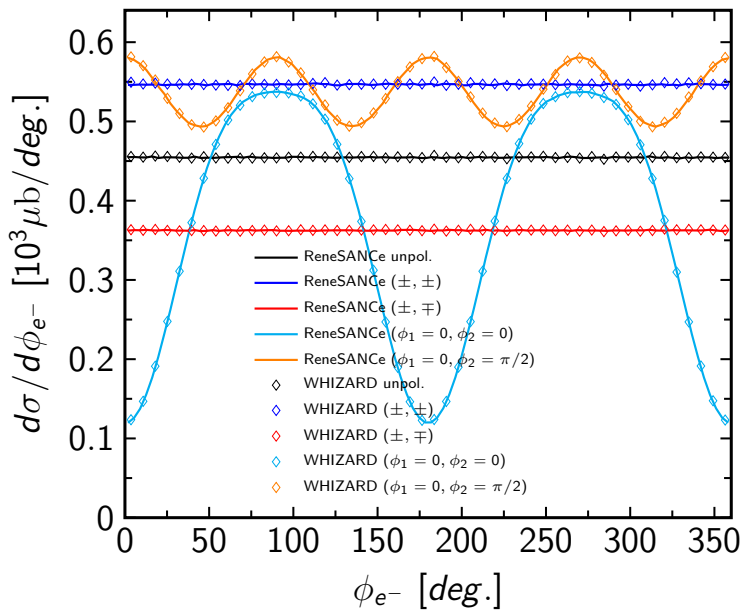
$\gamma\gamma \to e^+e^-$ cross sections for different polarization



Application for a photon collider at $\sqrt{S_{\gamma\gamma}} \sim 1$ MeV

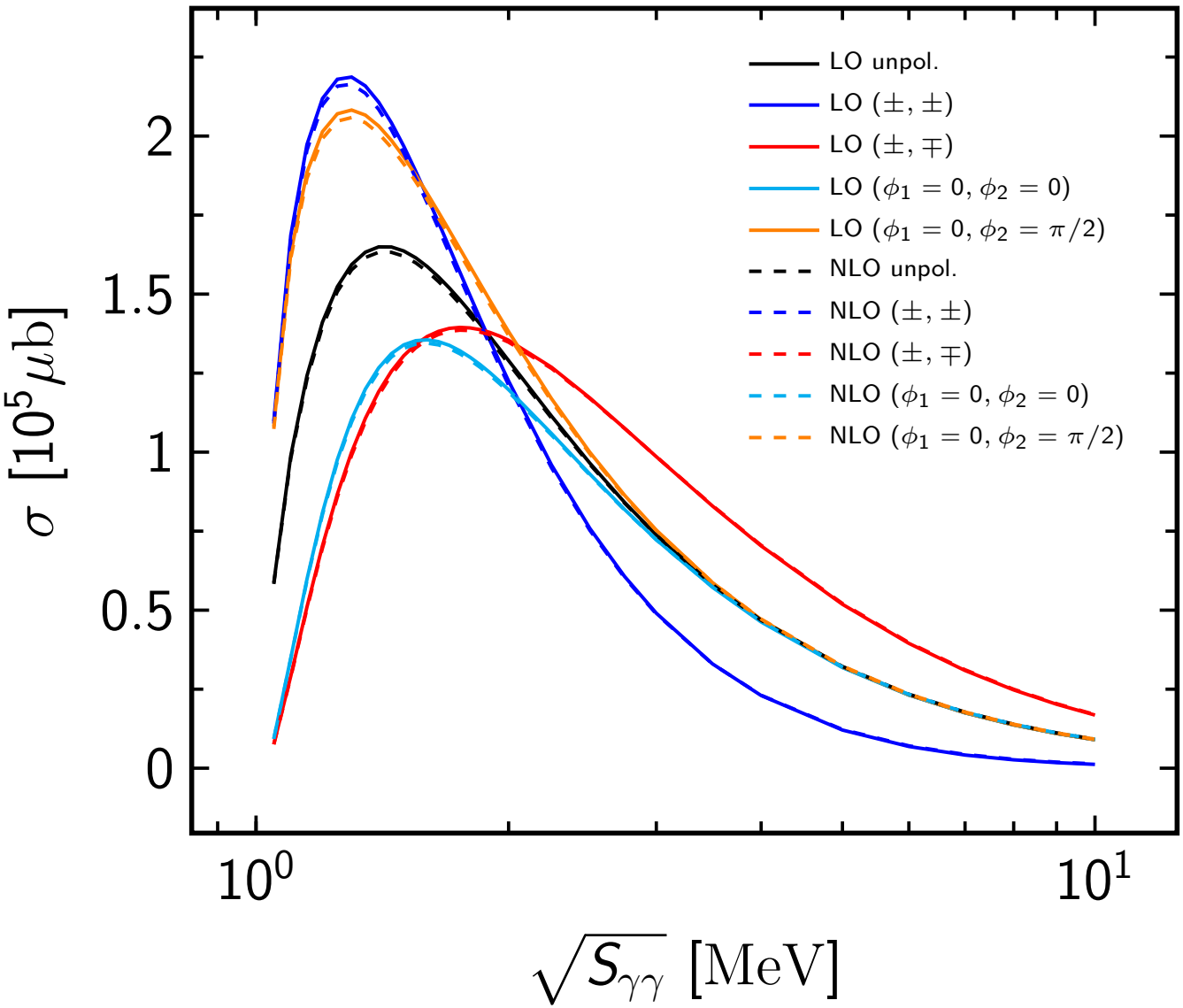
$\gamma\gamma \to e^+e^-$ cross sections for different polarization at $\sqrt{S_{\gamma\gamma}} = 1.5$ MeV





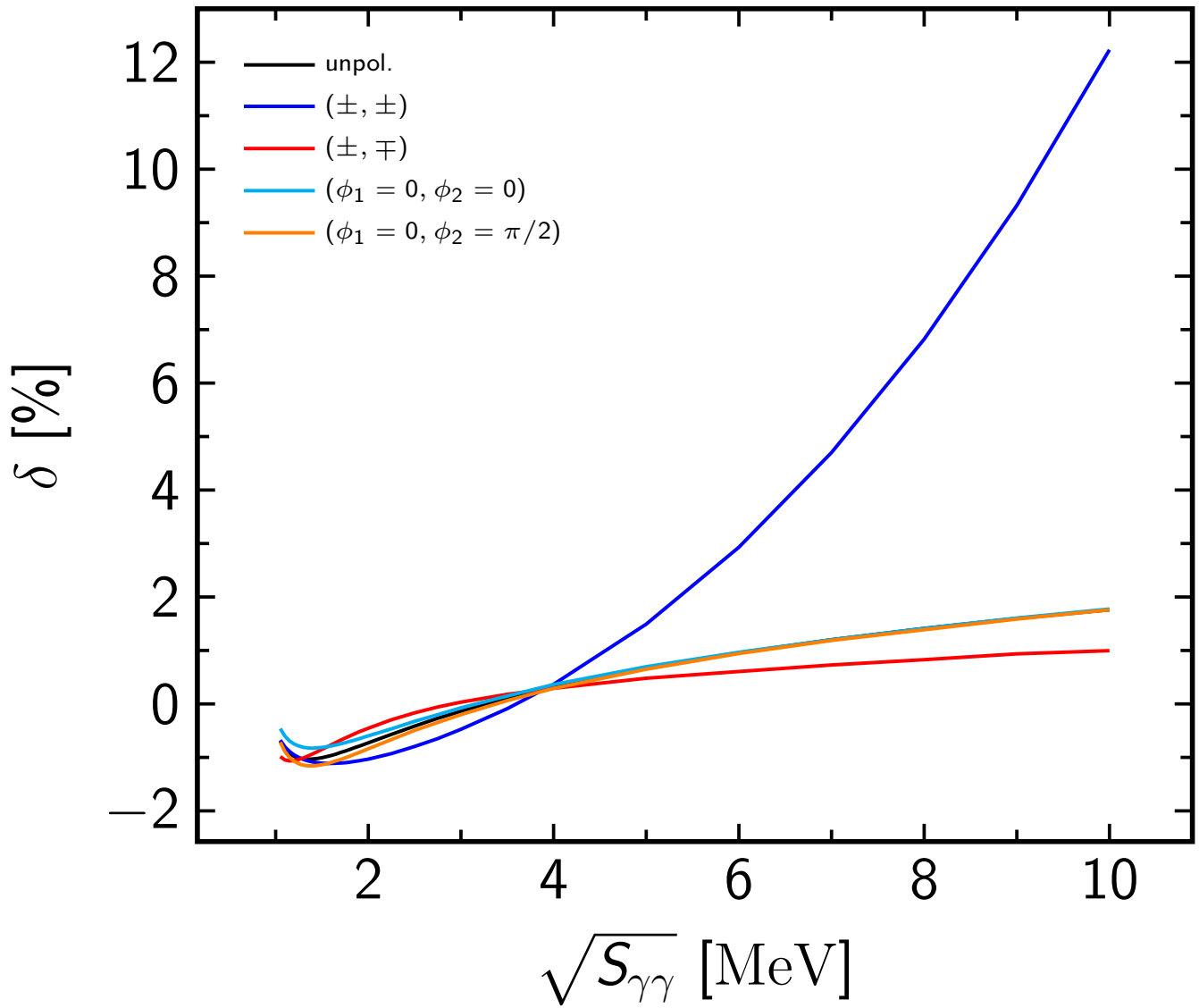
Application for a photon collider at $\sqrt{S_{\gamma\gamma}} \sim 1$ MeV

$\gamma\gamma \to e^+e^-$ cross sections for different polarization



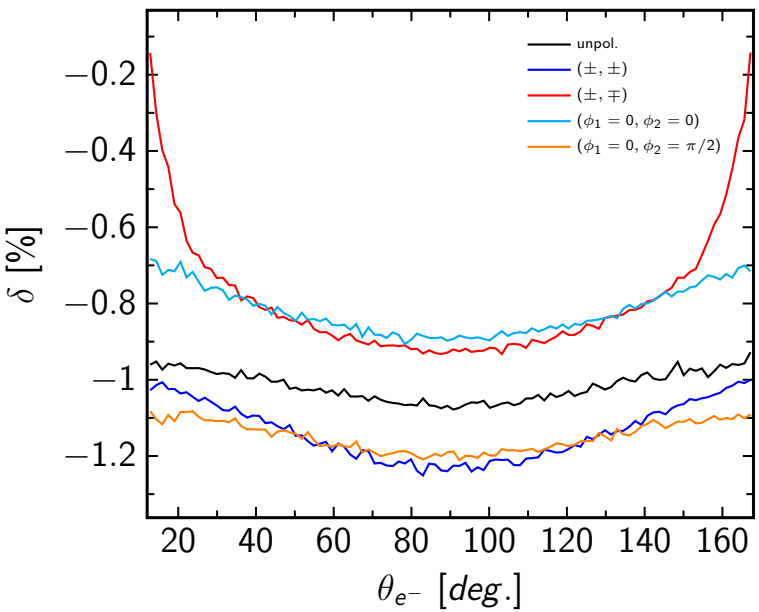
Application for a photon collider at $\sqrt{S_{\gamma\gamma}} \sim 1$ MeV

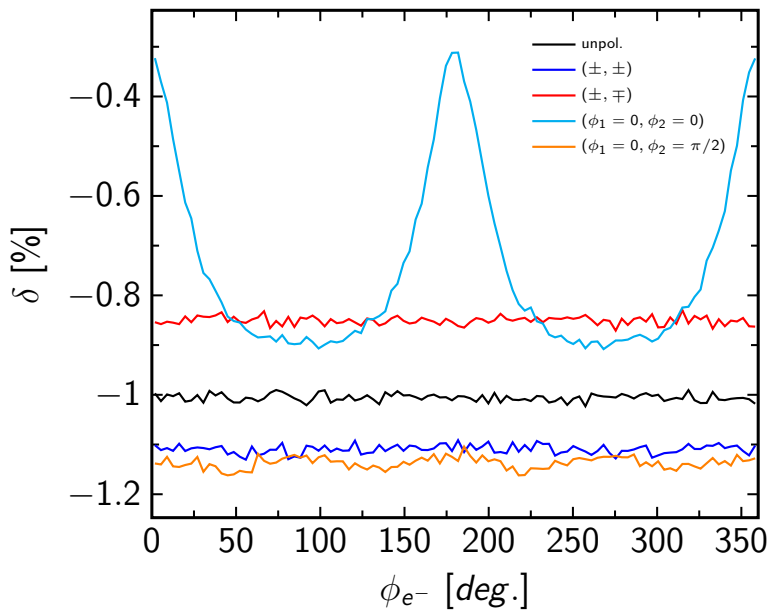
$\gamma\gamma \to e^+e^-$ cross sections for different polarization



Application for a photon collider at $\sqrt{S_{\gamma\gamma}} \sim 1$ MeV

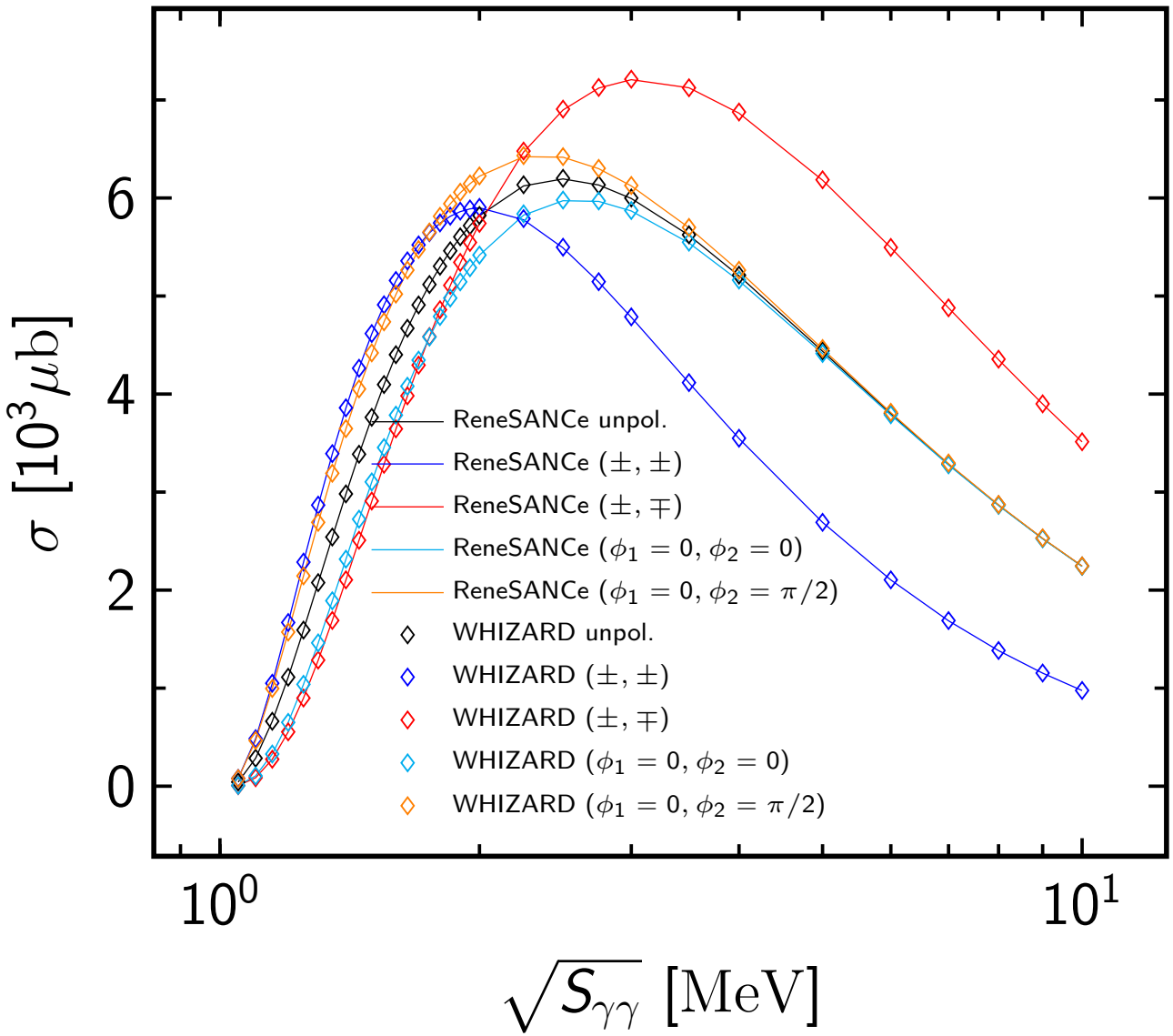
$\gamma\gamma \to e^+e^-$ cross sections for different polarization at $\sqrt{S_{\gamma\gamma}} = 1.5$ MeV





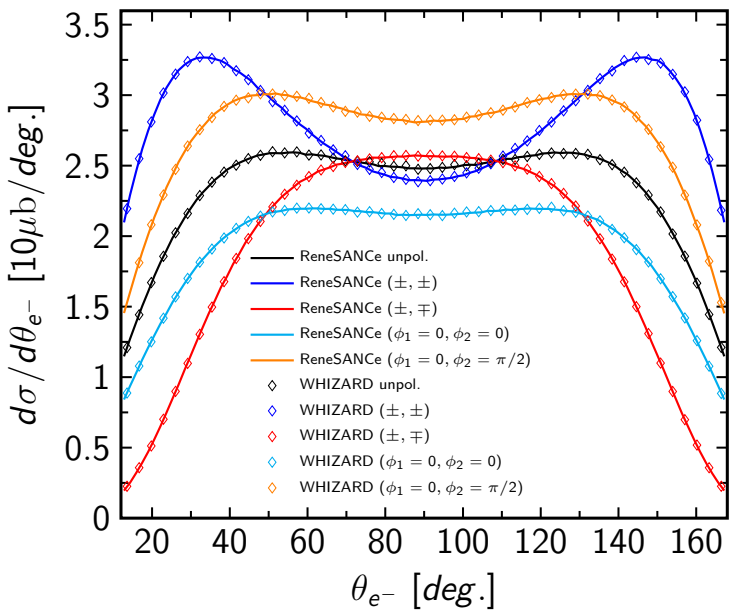
Application for a photon collider at $\sqrt{S_{\gamma\gamma}} \sim 1$ MeV

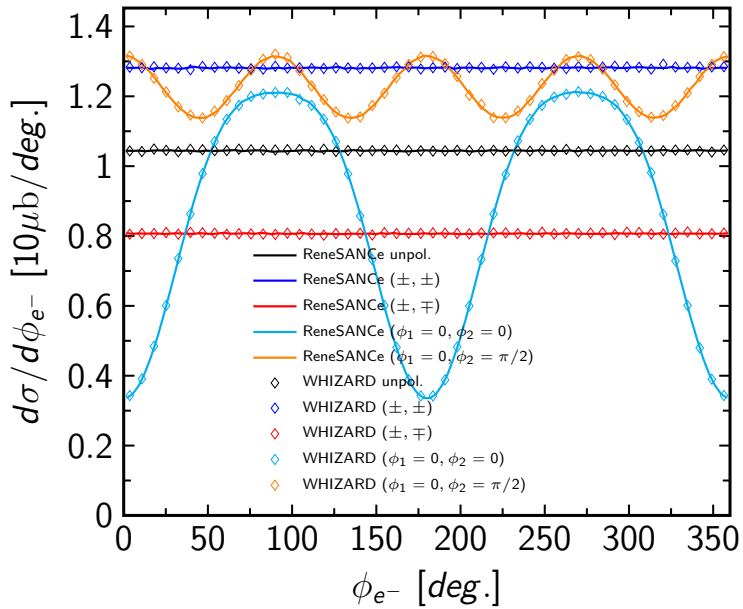
$\gamma\gamma \to e^+e^-\gamma$ cross sections for different polarization



Application for a photon collider at $\sqrt{S_{\gamma\gamma}} \sim 1$ MeV

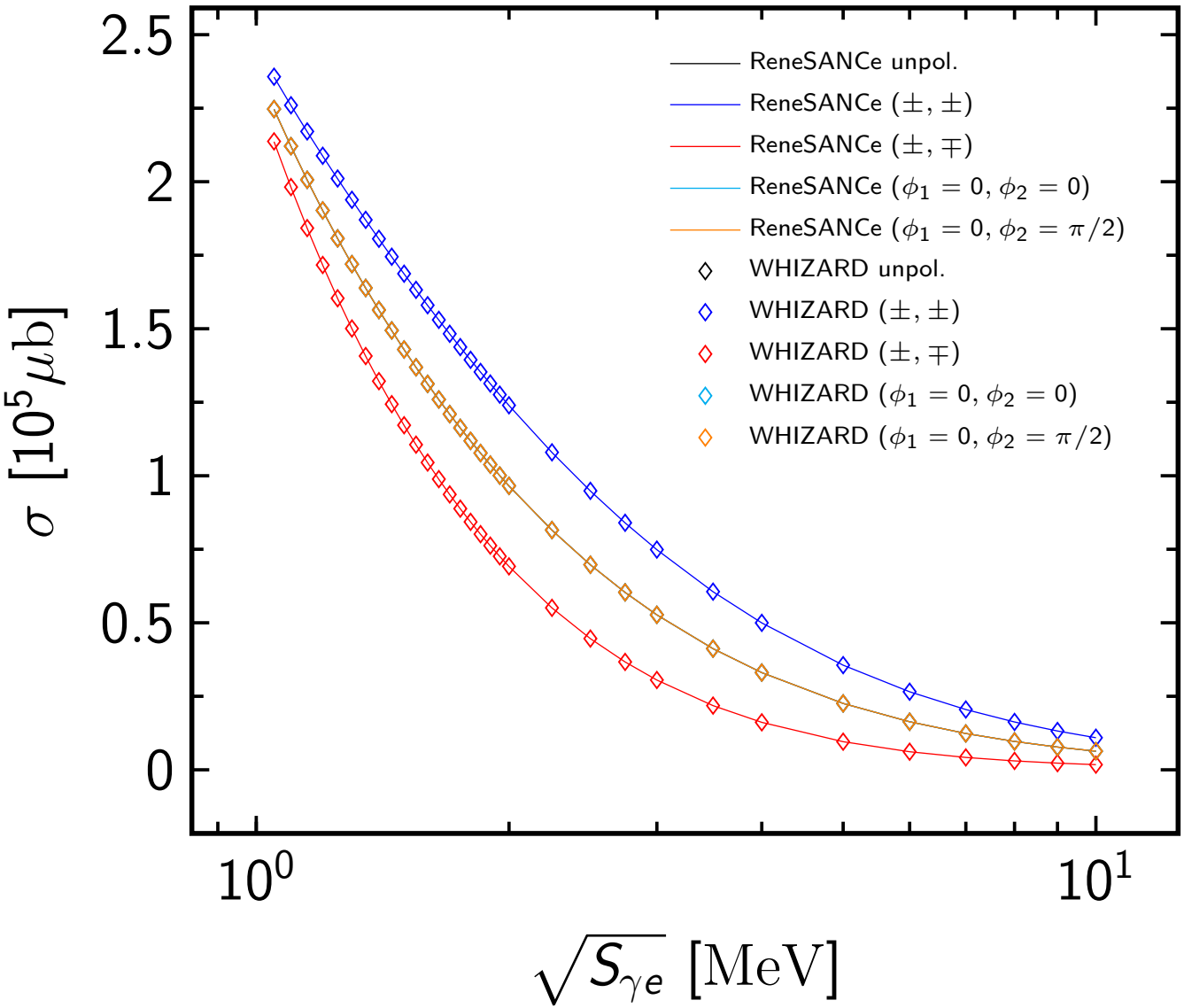
$\gamma\gamma \to e^+e^-\gamma$ cross sections for different polarization at $\sqrt{S_{\gamma\gamma}} = 1.5$ MeV





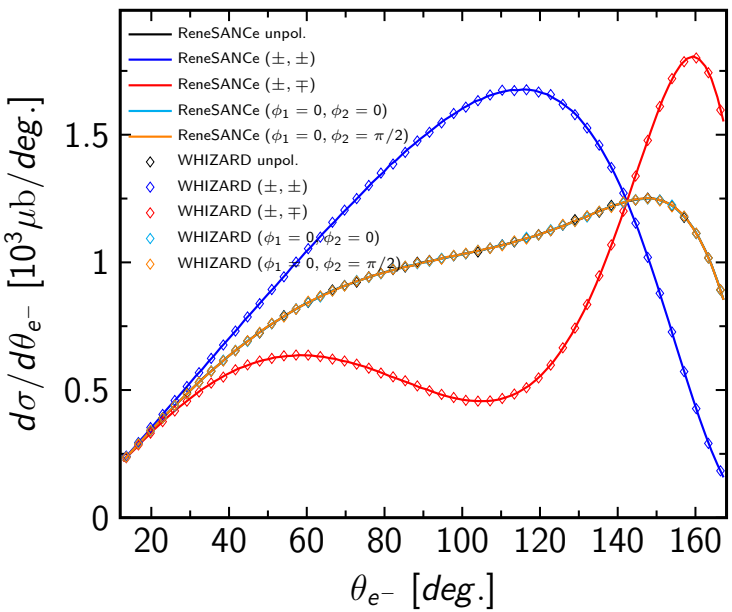
Application for a photon collider at $\sqrt{S_{\gamma\gamma}} \sim 1$ MeV

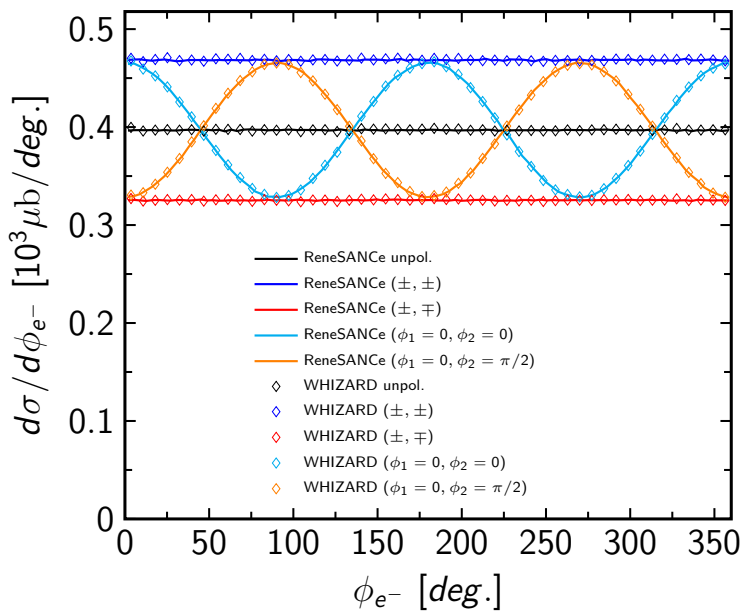
$e^-\gamma \to e^-\gamma$ cross sections for different polarization



Application for a photon collider at $\sqrt{S_{\gamma\gamma}} \sim 1$ MeV

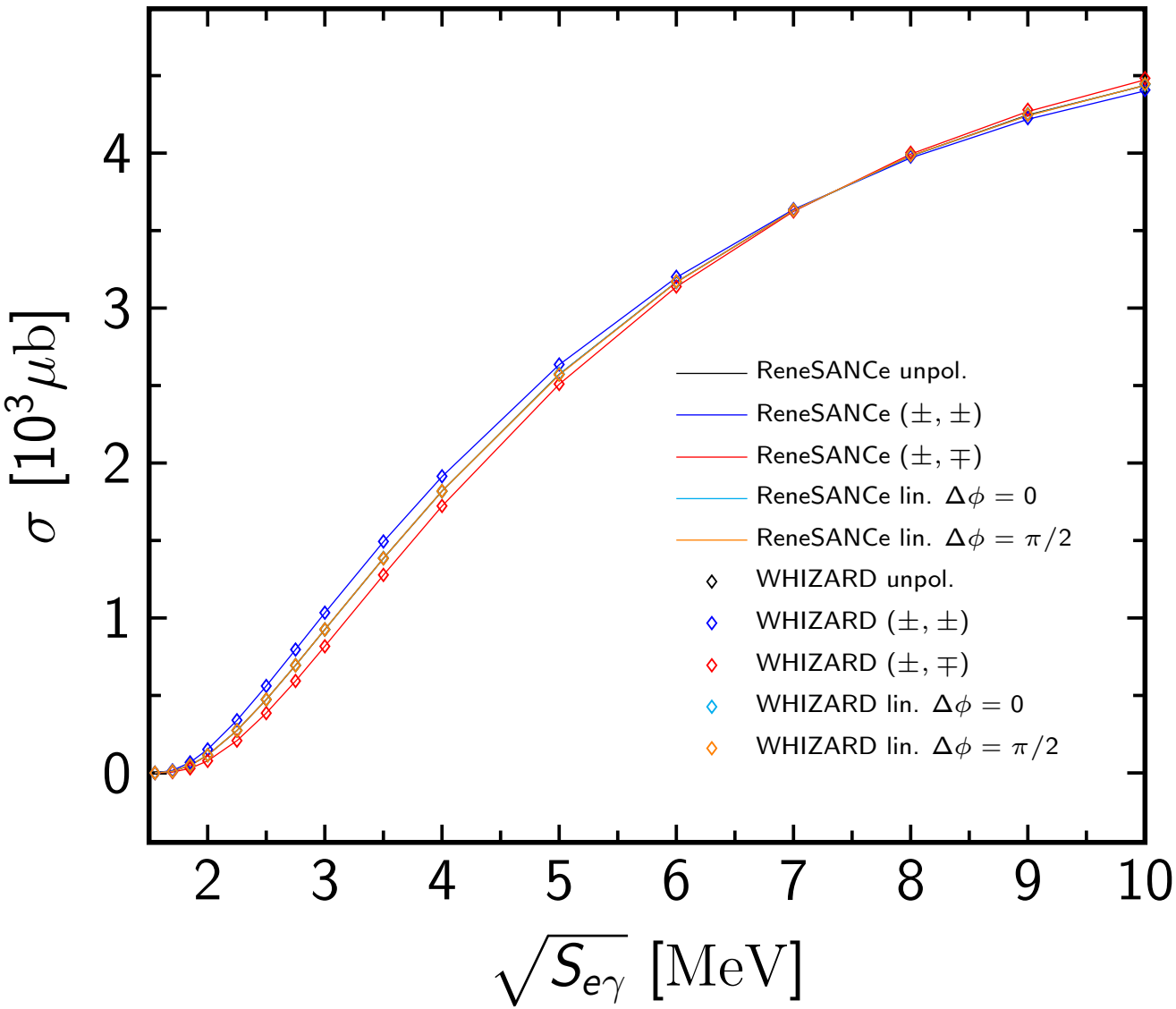
$e^-\gamma \to e^-\gamma$ cross sections for different polarization at $\sqrt{S_{e\gamma}} = 1.5$ MeV





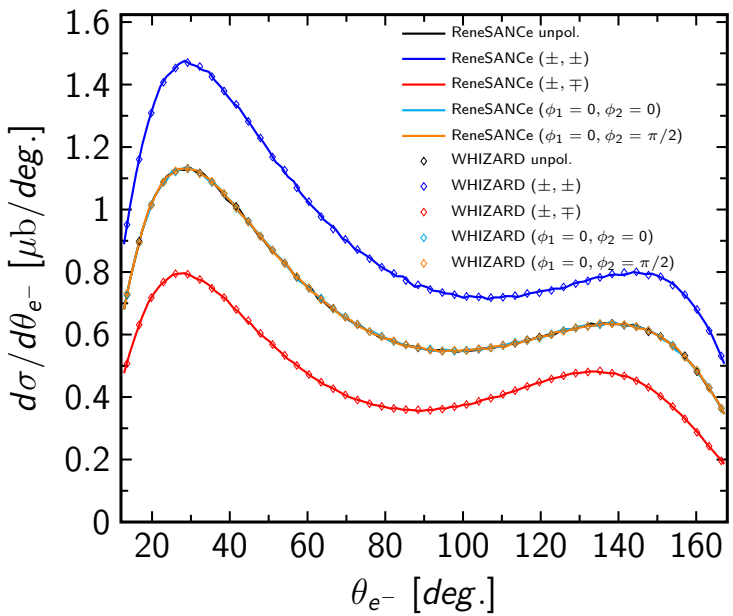
Application for a photon collider at $\sqrt{S_{\gamma\gamma}} \sim 1$ MeV

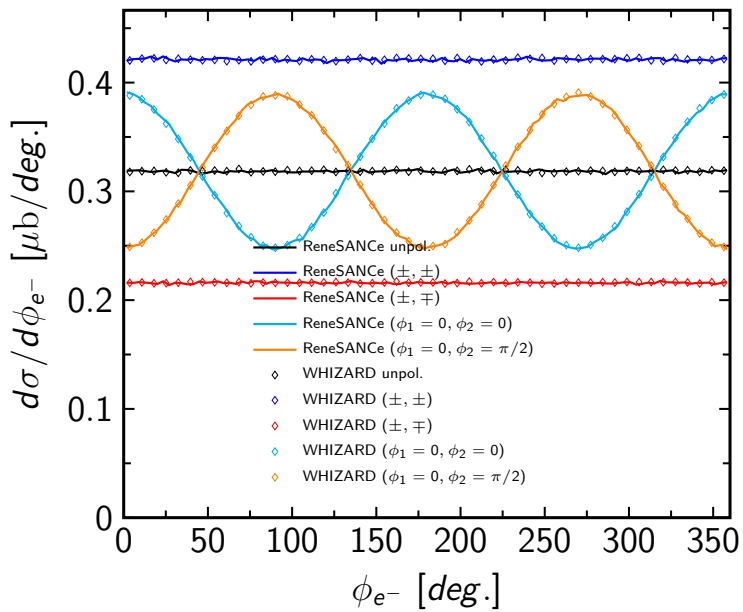
$e^-\gamma \to e^-e^+e^-$ cross sections for different polarization



Application for a photon collider at $\sqrt{S_{\gamma\gamma}} \sim 1$ MeV

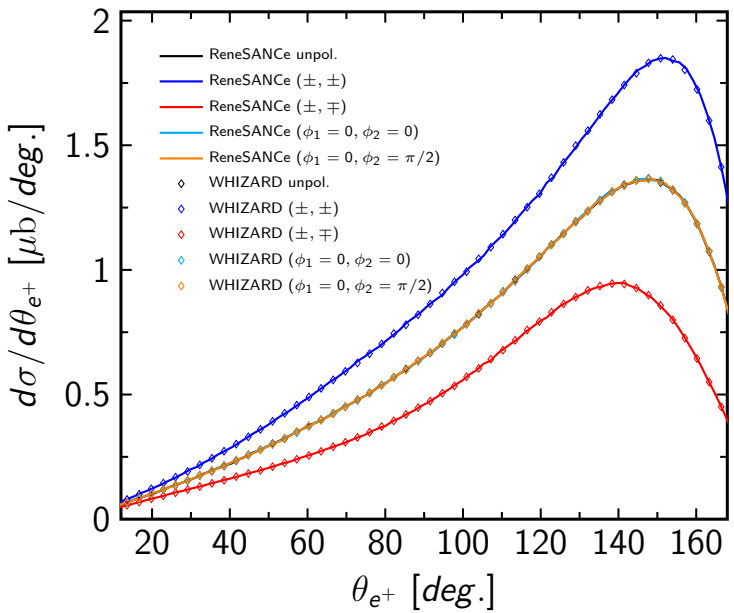
$e^-\gamma \to e^-e^+e^-$ cross sections for different polarization at $\sqrt{S_{e\gamma}} = 2$ MeV

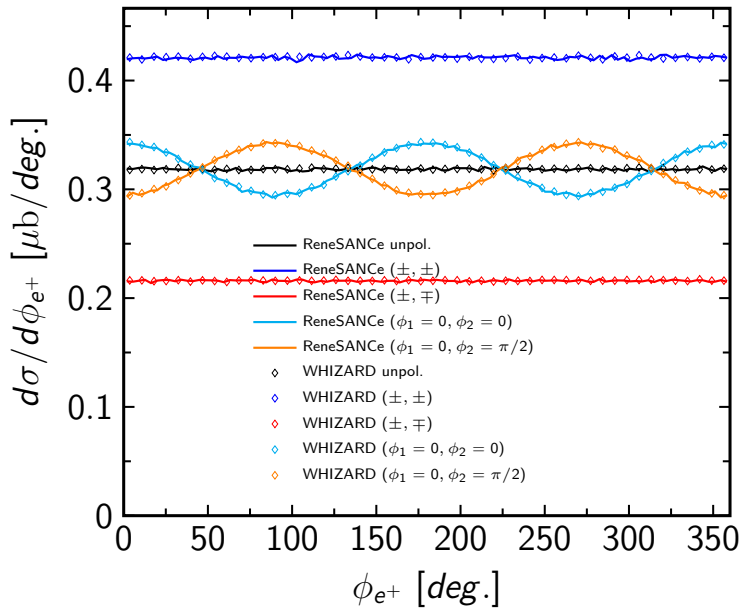




Application for a photon collider at $\sqrt{S_{\gamma\gamma}} \sim 1$ MeV

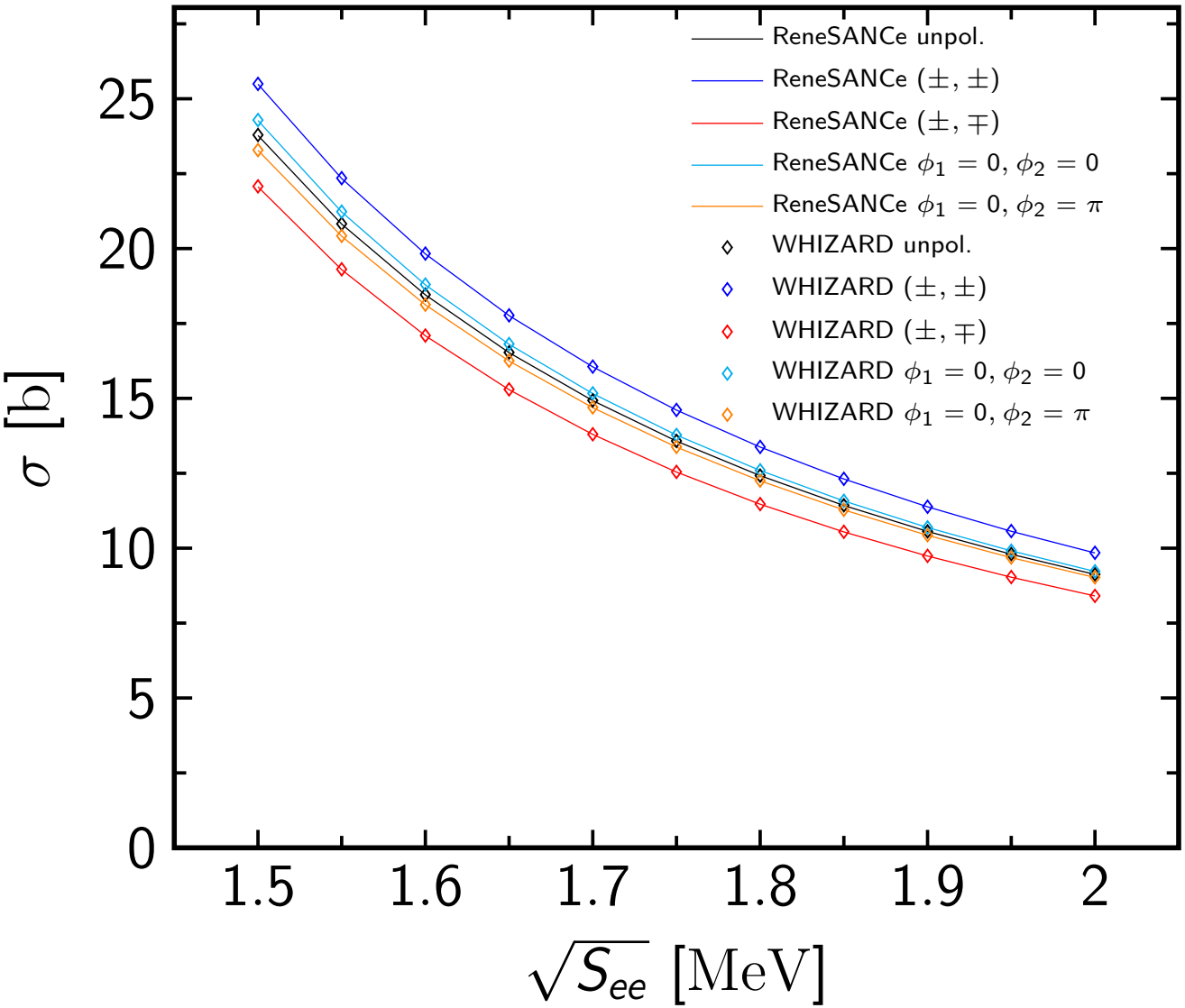
$e^-\gamma \to e^-e^+e^-$ cross sections for different polarization at $\sqrt{S_{e\gamma}} = 2$ MeV





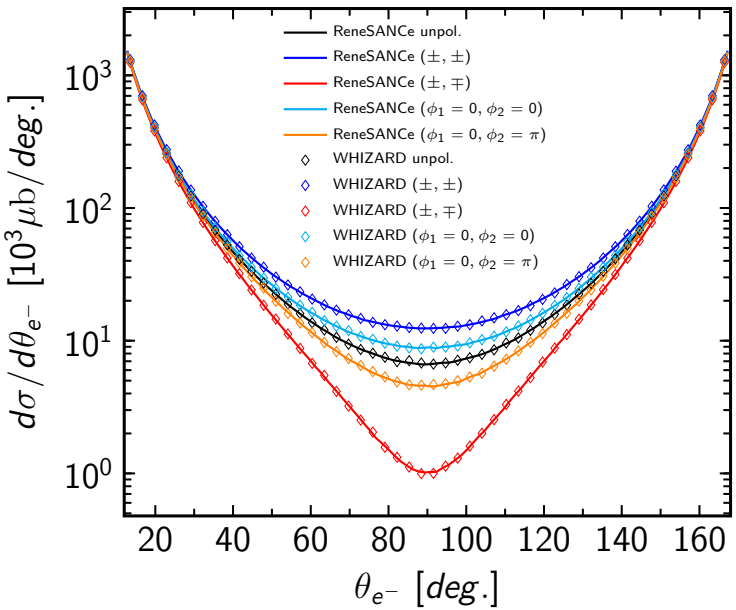
Application for a photon collider at $\sqrt{S_{\gamma\gamma}} \sim 1$ MeV

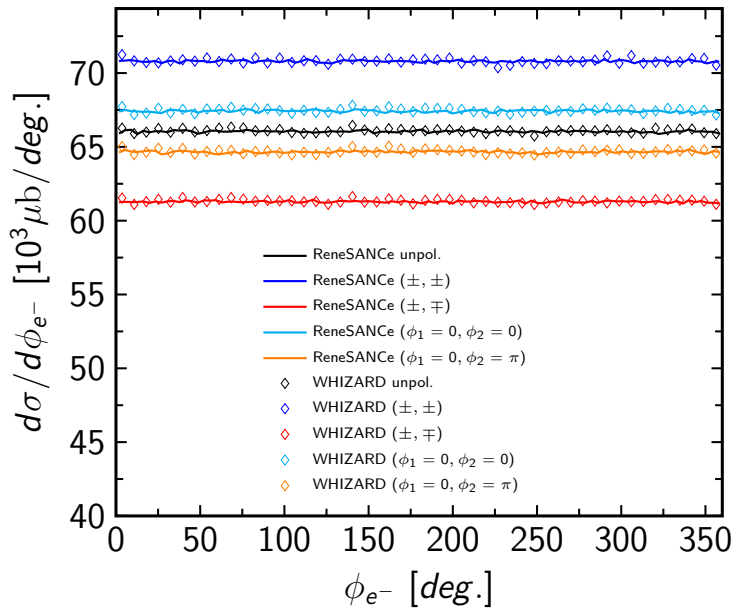
$e^-e^- \to e^-e^-$ cross sections for different polarization



Application for a photon collider at $\sqrt{S_{\gamma\gamma}} \sim 1$ MeV

$e^-e^- \to e^-e^-$ cross sections for different polarization at $\sqrt{S_{ee}} = 1.5$ MeV

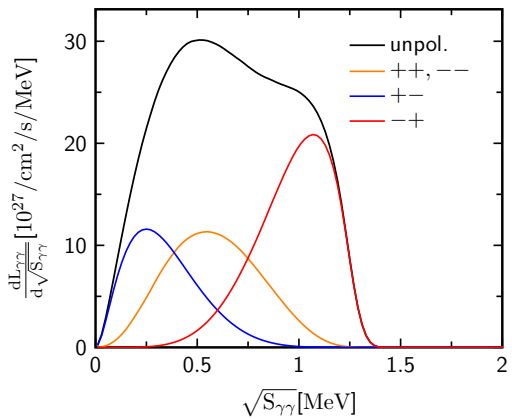




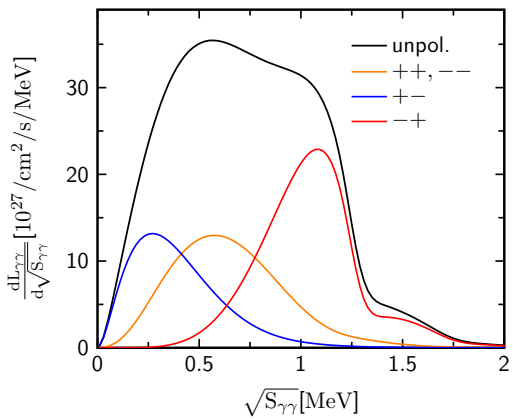
Application for photon collider at $\sqrt{S_{\gamma\gamma}} \sim 1$ MeV

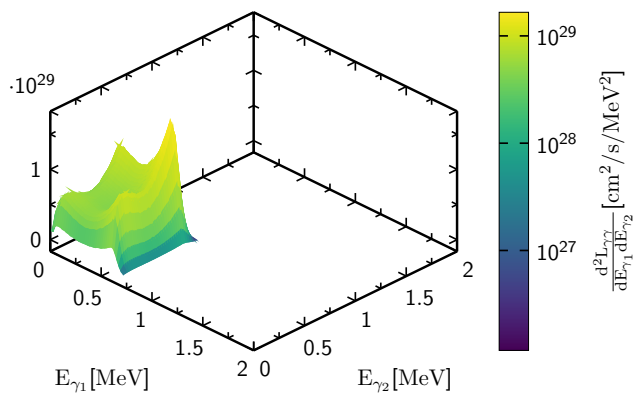
$\gamma\gamma$ luminosity $\mathcal{L}_{\gamma\gamma}$ simulated with CAIN 2.42

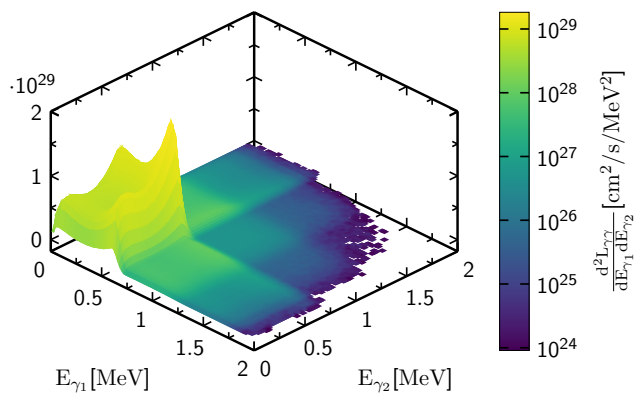
linear ICS



nonlinear ICS



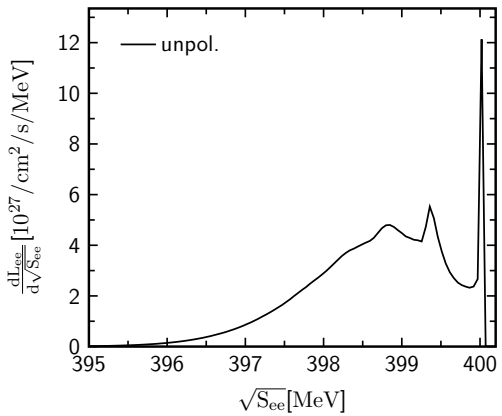


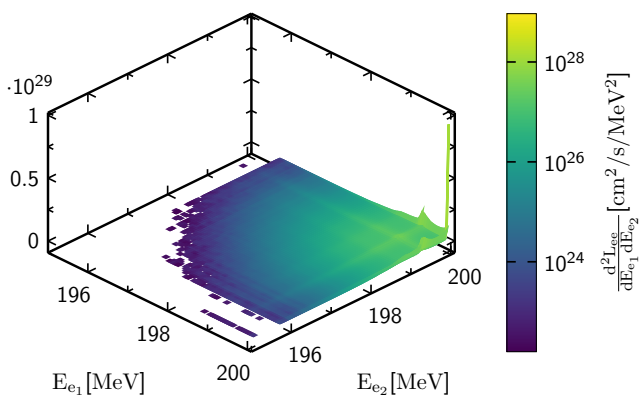


Application for photon collider at $\sqrt{S_{ee}} \sim 1$ MeV

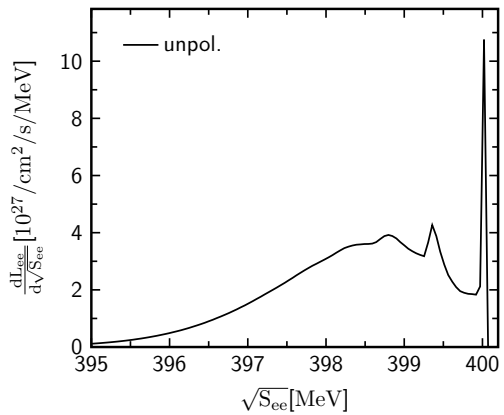
e^-e^- luminosity $\mathcal{L}_{ee}$ simulated with CAIN 2.42

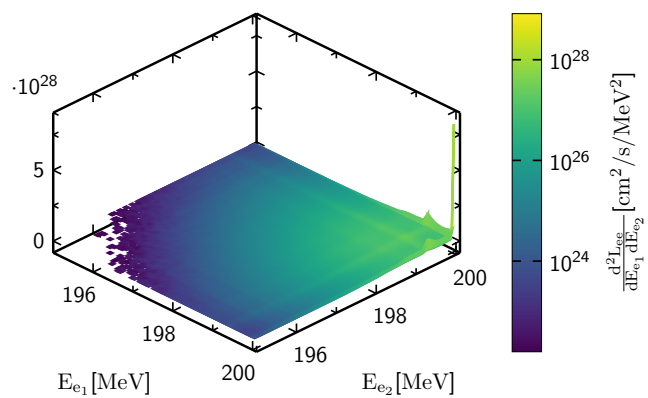
linear ICS





nonlinear ICS

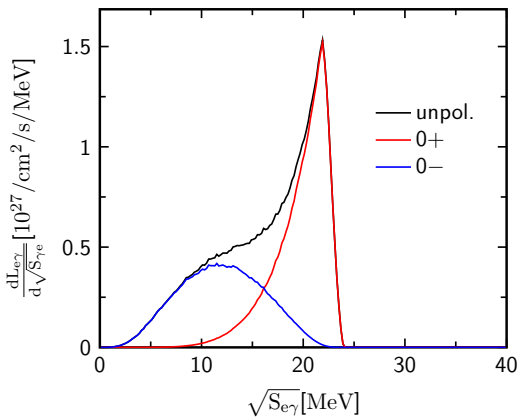


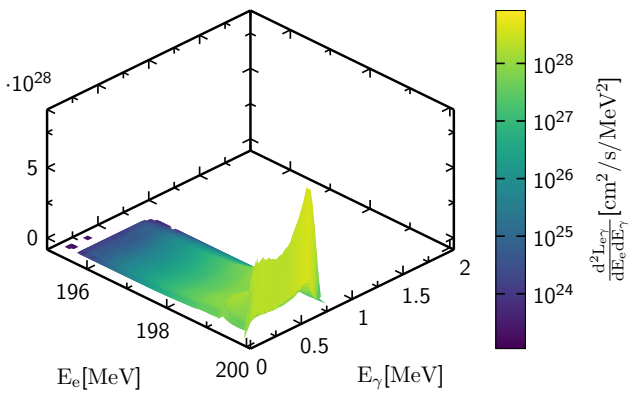


Application for photon collider at $\sqrt{S_{ee}} \sim 1$ MeV

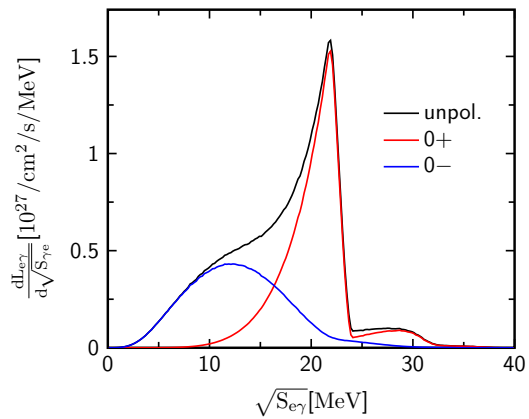
$e^-\gamma$ luminosity $\mathcal{L}_{e\gamma}$ simulated with CAIN 2.42

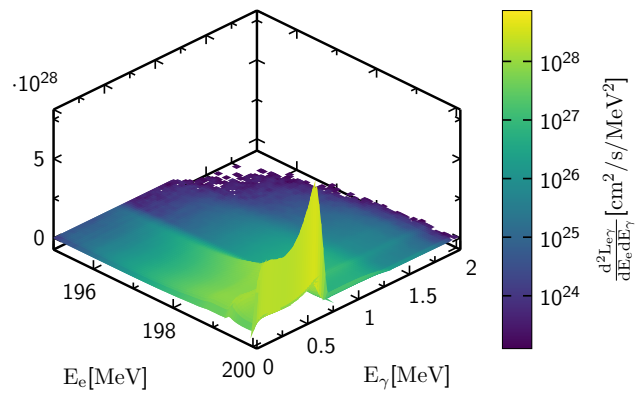
linear ICS





nonlinear ICS

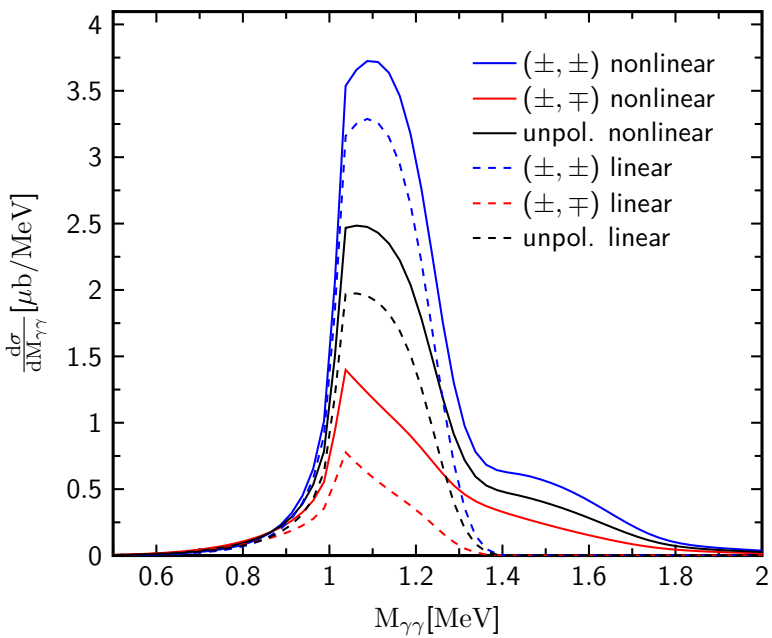


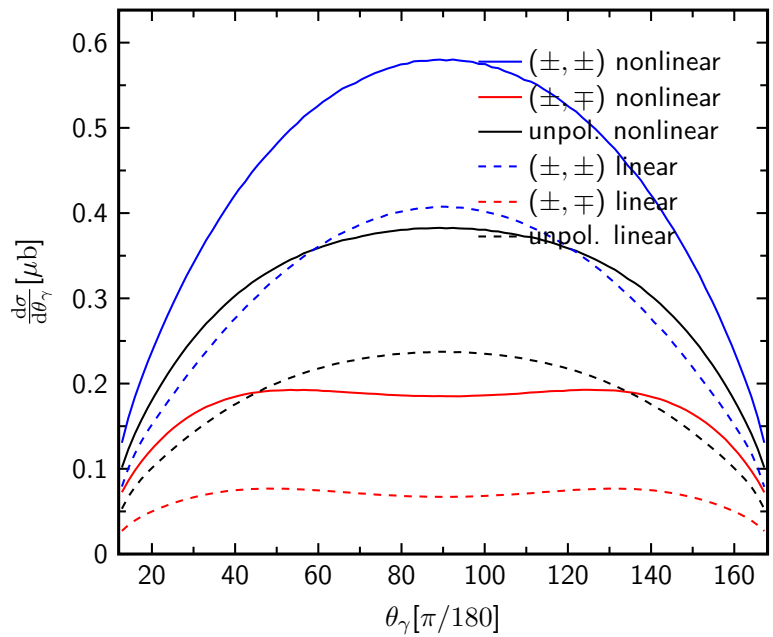


Application for photon collider at $\sqrt{S_{\gamma\gamma}} \sim 1$ MeV

The photon spectrum is simulated by CAIN 2.42 program and interfaced to ReneSANCe generator

$\gamma\gamma \to \gamma\gamma$

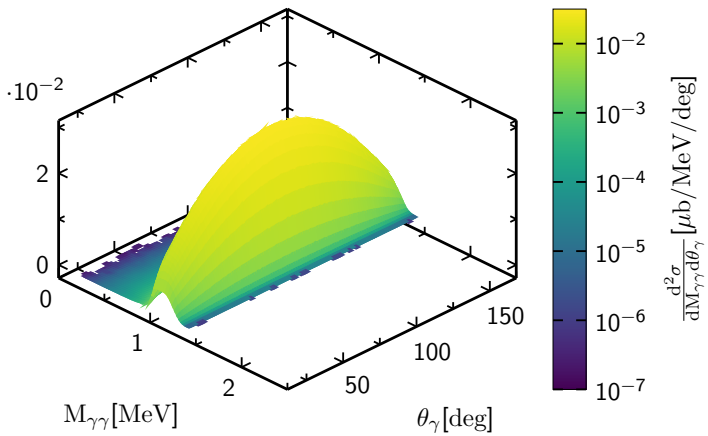




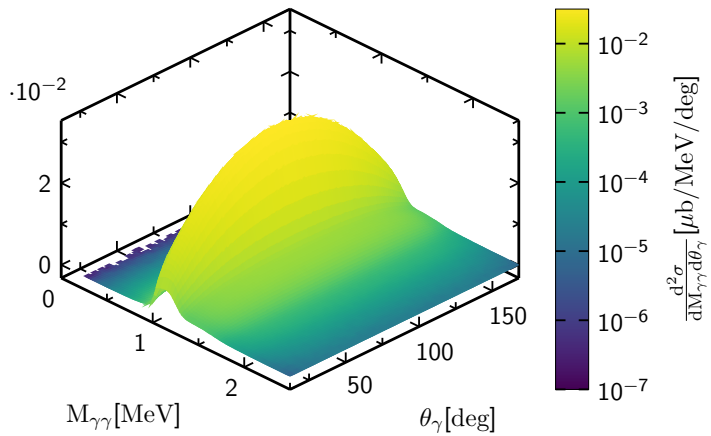
Application for photon collider at $\sqrt{S_{\gamma\gamma}} \sim 1$ MeV

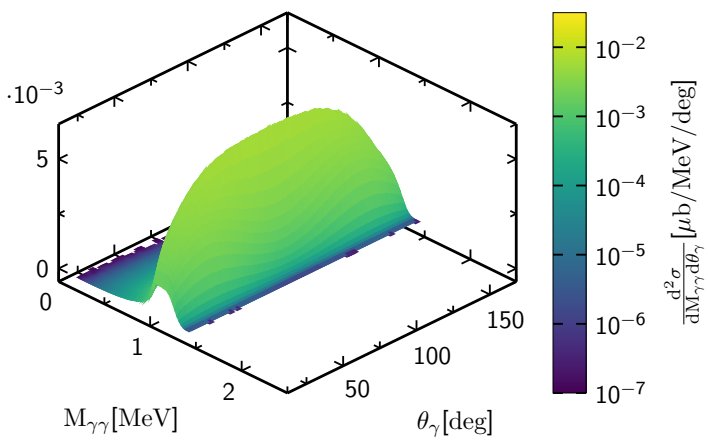
$\gamma\gamma \to \gamma\gamma$ cross section [upper: $(\pm, \pm)$, lower: $(\pm, \mp)$]

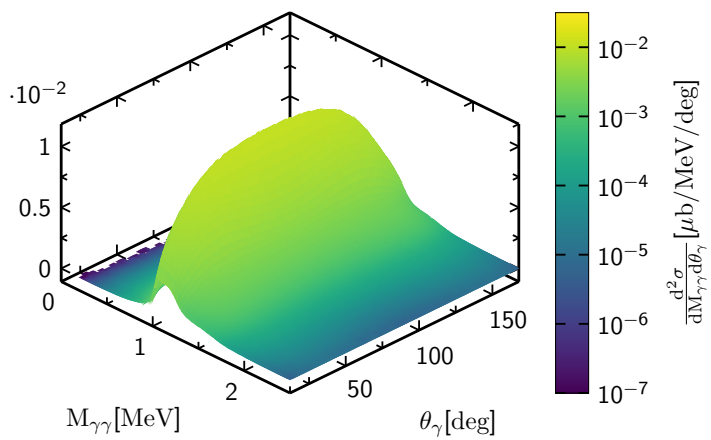
linear ICS



nonlinear ICS



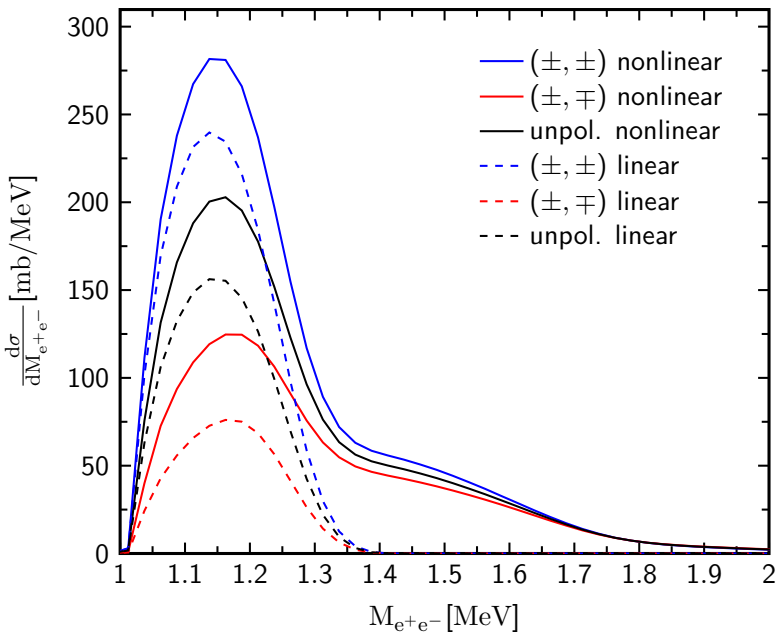


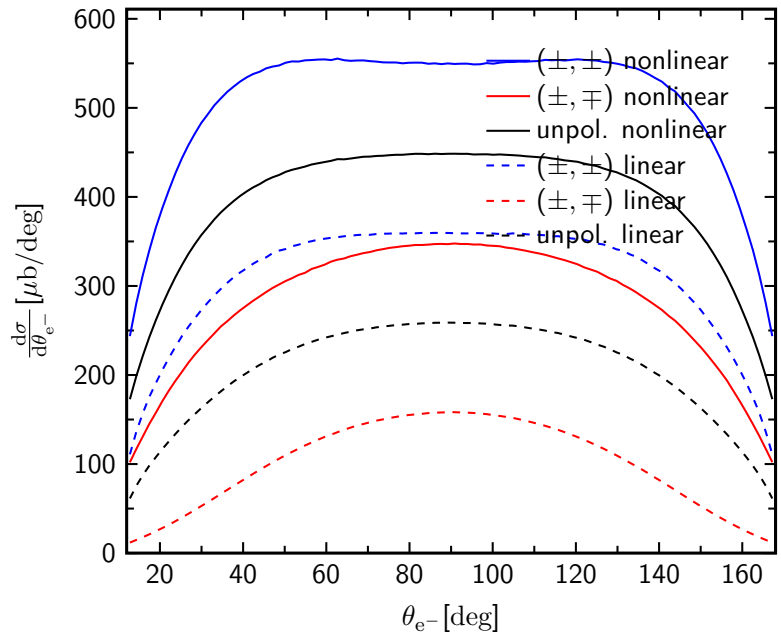


Application for photon collider at $\sqrt{S_{\gamma\gamma}} \sim 1$ MeV

The photon spectrum is simulated by CAIN 2.42 program and interfaced to ReneSANCe generator

$$\gamma\gamma \to e^+e^-$$

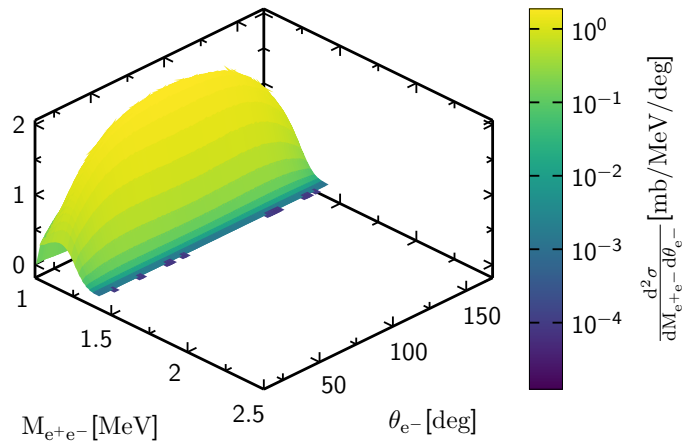




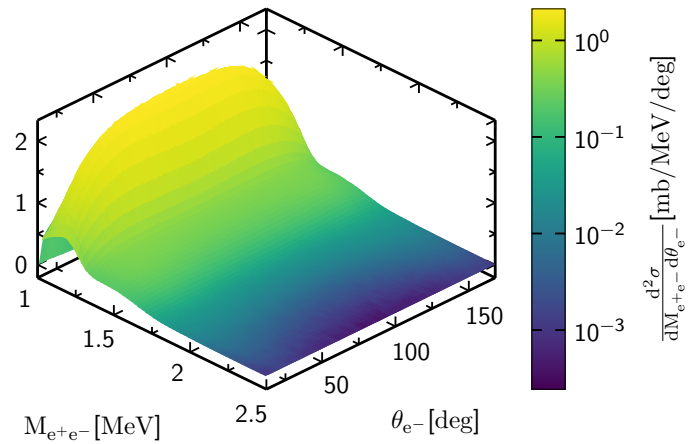
Application for photon collider at $\sqrt{S_{\gamma\gamma}} \sim 1$ MeV

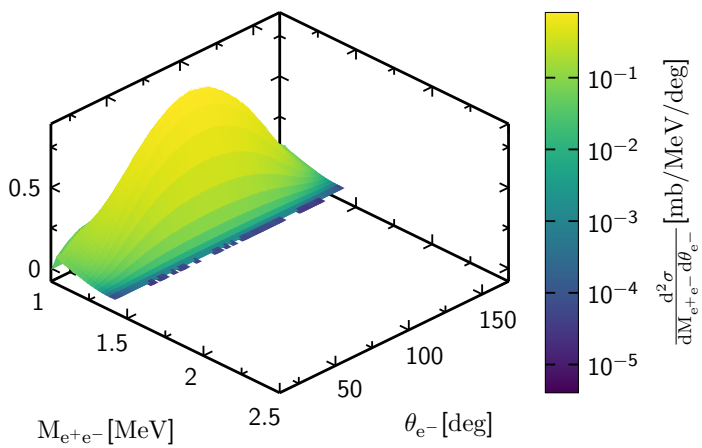
$\gamma\gamma \to e^+e^-$ cross section [upper: $(\pm,\pm)$, lower: $(\pm,\mp)$]

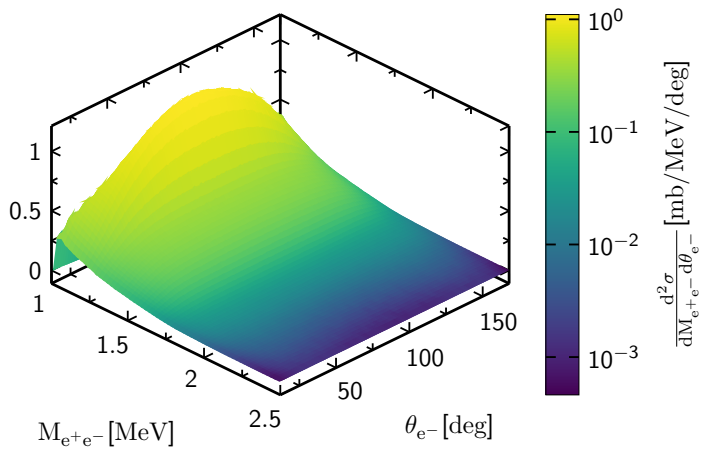
linear ICS



nonlinear ICS







Summary and plans

$\gamma\gamma$ collisions implemented in Monte Carlo event generator ReneSANCe

- $\gamma\gamma \to \gamma\gamma, \gamma Z, ZZ, e^+e^-$,
  $e^-e^- \to e^-e^-$, $e^-\gamma \to e^-\gamma$, $e^-\gamma \to e^-e^+e^-$ with arbitrary polarization of initial photons and electorns
- Events with unit weights, output in LHE, HepMC, HEPEVT and root formats
- Different options for $\gamma\gamma$ spectrum:
  - Simple model for liniear ICS
  - Interface to CAIN program
  - EPA spectrum in ultraperipheral heavy-ion collisions

Plans:

- New processes: $\gamma\gamma \to \nu\bar{\nu}, \ell^+\ell^-, t\bar{t}, W^+W^-, ZH$
- Massive two-loop QCD and QED corrections to $\gamma\gamma \to \gamma\gamma$
- Virtual photons

Thank you!